A multi-physics modelling approach to the dynamics of Molten Salt Reactors

Antonio Cammi, Valentino Di Marcello [1], Lelio Luzzi *, Vito Memoli, Marco Enrico Ricotti

Politecnico di Milano – Department of Energy, CeSNEF (Enrico Fermi Center for Nuclear Studies), via Ponzio 34/3 – 20133 Milano, Italy

ABSTRACT

This paper presents a multi-physics modelling (MPM) approach developed for the study of the dynamics of the Molten Salt Reactor (MSR), which has been reconsidered as one of the future nuclear power plants in the framework of the Generation IV International Forum for its several potentialities. The proposed multi-physics modelling is aimed at the description of the coupling between heat transfer, fluid dynamics and neutronics characteristics in a typical MSR core channel, taking into account the spatial effects of the most relevant physical quantities. In particular, as far as molten salt thermo-hydrodynamics is concerned, Navier–Stokes equations are used with the turbulence treatment according to the RANS (Reynolds Averaged Navier–Stokes) scheme, while the heat transfer is taken into account through the energy balance equations for the fuel salt and the graphite. As far as neutronics is concerned, the two-group diffusion theory is adopted, where the group constants (computed by means of the neutron transport code NEWT of SCALE 5.1) are included into the model in order to describe the neutron flux and the delayed neutron precursor distributions, the system time constants, and the temperature feedback effects of both graphite and fuel salt. The developed MPM approach is implemented in the unified simulation environment offered by COMSOL Multiphysics®, and is applied to study the behaviour of the system in steady-state conditions and under several transients (i.e., reactivity insertion due to control rod movements, fuel mass flow rate variations due to the change of the pump working conditions, presence of periodic perturbations), pointing out some advantages offered with respect to the conventional approaches employed in literature for the MSRs.

© 2011 Elsevier Ltd. All rights reserved.

1. Introduction

The interest of Generation IV International Forum (GIF) (GIF, 2002, 2008) for the Molten Salt Reactor (MSR), included in the six reactor concepts suggested for a sustainable nuclear energy development, encouraged many research groups to put renewed efforts in the study of the capabilities and physics of this system, which is featured by a liquid circulating fuel that also serves as coolant (Forsberg et al., 2003, 2007; Hron et al., 2006). The concept was initially proposed by Oak Ridge National Laboratory (ORNL) in the projects of the Aircraft Reactor Experiment (ARE) and the Molten Salt Reactor Experiment (MSRE) (Bettis et al., 1957; Rosenthal et al., 1970b). Afterwards, different studies were carried out by ORNL on the basis of the positive experience of the MSRE and several concepts of MSRs were proposed for a large scale nuclear energy production. Despite the technical issue concerning the online chemical reprocessing of the fuel, MSRs are reconsidered nowadays by GIF because of their several potentialities when compared

with solid-fuelled reactors (Forsberg et al., 2003; Furukawa et al., 2008; Hejzlar et al., 2009; LeBlanc, 2009). One of these advantages is represented by the possibility to work with a low fissile inventory. Moreover, radiation damage does not constitute a constraint on fuel burn-up limit as for solid-fuelled cores. In addition, a fluid fuel permits to have a homogeneous core composition eliminating the complications connected to the refuelling strategy, which in conventional reactors comprises reshuffling of the fuel assemblies. As demonstrated in the MSRE, MSRs can operate with different fissile materials and additives in the liquid fuel, proving the possibility to transmute and burn nuclear waste such as plutonium, minor actinides and long-lived fission products. MSRs can be designed considering both thermal and fast neutron spectrum leading to a wide operation flexibility. The adoption of thorium fuel cycle allows MSRs to perform breeding of fissile material (^{233}U) in thermal neutron spectrum. The graphite-moderated single-fluid Molten Salt Breeder Reactor (MSBR), developed by ORNL in the 1970s (Robertson, 1971), is an example of such a configuration and was confirmed "to have the potential to be an excellent Generation IV system, particularly as far as sustainability is concerned" (Renault et al., 2005). In addition, this reactor constituted the starting point for the development of the project THORIMS-NES (Thorium Molten-Salt Nuclear Energy Synergetics), which is based on a

---

* Corresponding author. Tel.: +39 02 2399 6326; fax: +39 02 2399 6309.
 E-mail address: lelio.luzzi@polimi.it (L. Luzzi).
[1] Present address: European Commission, Joint Research Centre, Institute for Transuranium Elements, P.O. Box 2340, Karlsruhe, Germany.

Nomenclature

$a_0\ a_1\ a_2$	coefficients defined by Eq. (14)
b	coefficient of Eq. (20)
c_i	concentration of the ith precursor group
C_P	specific heat
$C_{\varepsilon 1}$	k–ε model empirical constant
$C_{\varepsilon 2}$	k–ε model empirical constant
C_μ	k–ε model empirical constant
D	neutron diffusion coefficient
$F_\perp$	horizontal component of volume force
$F_{//}$	vertical component of volume force
g	gravity acceleration
H	axial channel length
I	identity matrix
k	turbulent kinetic energy
K	thermal conductivity
K_T	turbulent thermal conductivity, $\{=C_{P,F}\eta_T/\mathrm{Pr}_T\}$
n	integer number
p	fluid pressure
pcm	per cent mille $\{=10^{-5}\}$
P	power generated by the analysed core channel
P_0	nominal power generated by the analysed core channel
Pr	molecular Prandtl number
Pr_T	turbulent Prandtl number
Q	heat source
r	radial coordinate
R_1	channel radius/inner radius of graphite
R_2	outer radius of graphite
R_G	symmetry radius of graphite
t	time
t_0	reference time
T	temperature
T_0	reference temperature
T^{av}	average temperature
u	velocity vector
u_r	velocity along the radial direction
u_z	velocity along the axial direction
v	neutron velocity
z	axial coordinate

Greek symbols

α	volume thermal expansion coefficient of fuel salt
α_T	temperature reactivity feedback coefficient
β	total delayed neutron fraction, $\{=\sum_{i=1}^{6}\beta_i\}$
β_i	delayed neutron fraction of the ith precursor group
γ	fraction of the heat in the fuel generated into graphite
Γ	fuel salt mass flow rate
Γ_0	fuel salt mass flow rate at nominal conditions
$\delta\Sigma(z,t)$	cross section local perturbation
Δz	axial size of the fissile lump
ε	turbulent dissipation rate
ε_f	heat produced per fission reaction
η	fuel salt dynamic viscosity
η_T	eddy viscosity, $\{=\rho_F C_\mu k^2/\varepsilon\}$
Θ	Heaviside function
λ_i	decay constant of the ith precursor group
v	average number of neutrons per fission
ρ	density
ρ_0	fluid density at reference temperature
σ_ε	k–ε model empirical constant
σ_k	k–ε model empirical constant
Σ	neutron cross section
Σ^0	unperturbed cross section
Σ_a	absorption cross section
Σ_{abs}	control absorption cross section
Σ_f	fission cross section
$\Sigma_{1\rightarrow 2}$	down-scattering cross section
$\Sigma_{2\rightarrow 1}$	up-scattering cross section
τ	fuel recirculation time $\{=\tau_C + \tau_{EL}\}$
τ_C	residence time in the core
τ_{EL}	residence time in the external primary loop (out of the core)
φ	neutron flux

Subscripts

F	fuel salt
G	graphite
1	fast neutron group
2	thermal neutron group
in	inlet
out	outlet

symbiotic system coupling fission with spallation, with several advantages in terms of proliferation resistance, safety, fuel cycle, radioactive waste management, economics and resources (Furukawa et al., 2008).

In MSRs, the unusual characteristic of fluid fuelled core shows itself in the form of a strong non-linear coupling between the fuel motion and neutron dynamics, because delayed neutron precursors (DNP) created in the core can decay in a different position of the primary loop affecting the overall neutron balance (Lapenta, 2005; Nicolino et al., 2008). Besides, the fuel velocity field depends on the fission source term, which determines the temperature distribution in the fuel salt, and its density variations. For this reason, an accurate description of the dynamic behaviour of such a complex system should properly allow for the different physical phenomena, their coupling mechanisms and the related spatial effects.

In nuclear engineering, the coupling between neutronics and thermal–hydraulics has been studied and analysed for many years. Recently, thanks to a growing availability of computational resources, Coupled Code Techniques (CCT), which employ a Thermal–Hydraulic System Code (THSC) and a reactor Neutron Kinetics Code (NKC), are widely used, above all for safety analysis (Salah et al., 2008). In particular, two different approaches to couple THSC and 3D NKC exist, namely: the serial integration coupling (it requires modifications of the codes by implementing a subroutine for neutronics into the THSC), and the parallel processing coupling (codes run separately and exchange data during the calculation, involving minor modifications). Such approaches are well assessed for conventional nuclear reactors, but may result non-completely satisfactory in the case of MSRs, because the description of physical quantities (for instance, the unusual spatial distribution of delayed neutron precursors) would require drastic modifications of the numerical and mathematical structure of the software generally adopted for solid-fuelled reactors. In this context, the multi-physics modelling (MPM) looks very promising for the employment in the field of nuclear engineering as an integrative analysis support in the design development of current and innovative nuclear reactors (Cammi and Luzzi, 2008; Di Marcello, 2010; Memoli, 2010). Actually, the MPM prevents the employment of dedicated numerical tools and the modification of their numerical structure. This approach basically consists of a set of non-linear and time-dependent coupled partial differential equations (implemented in the same environment of simulation), which are

descriptive of the different physical phenomena occurring in a nuclear reactor, and in principle are applicable to a more or less complex domain with boundary conditions of general kind.

As concerns MSRs, the current research is aimed at investigating different descriptive approaches. Efforts in this sense were carried out by different authors and for a variety of molten salt systems adopting different hypotheses and simplifications (a literature overview is summarized in Table 1, and is briefly outlined here below). In each case, a dedicated code to the specific reactor of interest was implemented on purpose or extended from a previous code in order to include the fuel motion effect. Lapenta et al. (2001) analysed the neutronics for fluid fuel systems by means of a point-kinetics model, while Dulla et al. (2004) and Dulla and Ravetto (2007) used the quasi-static method (only a prescribed velocity field oriented in one direction was considered and no temperature cross section feedback was taken into account). Lecarpentier and Carpentier (2003) developed the Cinsf1D code to study the AMSTER system, in which a simplified 1D thermal–hydraulic and neutron diffusion model was adopted. Yamamoto et al. (2005, 2006) and Suzuki and Shimazu (2006, 2008) performed the steady-state and transient analyses for the SMSR (Small Molten Salt Reactor) by coupling the neutron diffusion equations with the heat transfer equations in fuel salt and graphite, in which the fluid flow model was solved in one-dimensional form through the use of some empirical formulas. Křepel et al. (2005, 2007) developed the DYN1D-MSR and DYN3D-MSR codes for performing transient analysis of the MSBR and MSRE, in which the neutron diffusion equations were adopted for neutronics calculation, and a one-dimensional flow model was used even in the 3D code. Wang et al. (2006) focused on the fluid dynamic simulation and optimization of the MOSART (Molten Salt Advanced Reactor Transmuter) core in steady-state conditions by means of an extension of the thermo-hydraulic and neutronic models of the SIMMER-III code. The coupled thermo-fluid and neutronic dynamics of MOSART was also researched by Nicolino et al. (2008), in which the stream function-vorticity was preferred for fluid motion and the diffusion theory was chosen for neutronics. Kópházi et al. (2009) set up a 3D time-dependent calculation scheme for the MSRE (by coupling the DALTON and THERM codes in an iterative manner), in which the fuel heat transfer in the core channels was simplified by using a correlation for the Nusselt number. Zhang et al. (2009a,b) performed transient and safety analyses for a generic single-fluid Molten Salt Reactor and the MOSART system, respectively, employing simplified heat transfer, neutronic and flow models. Successively, Zhang et al. (2009c) extended the models previously adopted (Zhang et al., 2009a,b) by means of a more refined modelling of fluid dynamics and neutronics, referring to steady-state conditions.

The above literature overview shows that most of the studies carried out on MSRs use rough flow models and hypotheses, such as assuming known velocities (Lapenta et al., 2001; Dulla et al., 2004; Dulla and Ravetto, 2007), one-dimensional flow and simplified heat transfer models (Lecarpentier and Carpentier, 2003; Křepel et al., 2005, 2007; Yamamoto et al., 2005, 2006; Suzuki and Shimazu, 2006, 2008; Kópházi et al., 2009; Zhang et al., 2009a,b), simple cross section feedback (Nicolino et al., 2008), only steady-state conditions (Wang et al., 2006; Zhang et al., 2009c). In order to provide a deeper insight into the steady-state and transient characteristics of MSRs, the present work proposes a multi-physics modelling (MPM) approach for the description of the coupling between neutronics and thermo-hydrodynamics by means of COMSOL Multiphysics® (COMSOL, 2008a). This approach was developed with the aim to study the dynamic behaviour of MSRs by taking into account the spatial effects of the most relevant physical quantities. In particular, as far as the molten salt thermo-hydrodynamics is concerned, Navier–Stokes equations are used with the turbulence treatment according to the Reynolds Averaged Navier–Stokes (RANS) scheme, while the heat transfer is taken into account through the energy balance equations for the fuel salt and the graphite. As far as neutronics is concerned, the two-group diffusion theory (Meem, 1964) is adopted, where the group constants are considered as input values

Table 1
Main modelling approaches to MSRs available in literature.

Author	Reactor	Geometry	Analysis type/code	Neutronics/fuel and graphite cross section treatment	Thermo-hydrodynamics
Lecarpentier and Carpentier (2003)	AMSTER	1-D	Transient Cinsf1D	Two-group diffusion theory Homogeneous approach	Prescribed uniform velocity field Empirical correlation for heat transfer fuel/graphite
Wang et al. (2006)	MOSART	2-D, axial-symmetric	Steady extension of SIMMER-III	Neutron kinetics model based on the improved quasi-static scheme Homogeneous approach	Navier–Stokes equations
Yamamoto et al. (2006)	SMSR	2-D, axial-symmetric	Transient	Two-group diffusion theory Heterogeneous approach	Navier–Stokes equations Empirical correlation for heat transfer fuel/graphite
Křepel et al. (2007, 2008)	MSRE and MSBR	3-D (neutronics) 1-D (thermal–hydraulics)	Transient DYN3D-MSR	Two-group diffusion theory Homogeneous approach	Navier–Stokes equations Empirical correlations for heat transfer fuel/graphite
Nicolino et al. (2008)	MOSART	2-D, axial-symmetric	Transient	Multi-group diffusion theory Generic cross sections as a function of the fuel density	Navier–Stokes equations (stream function/vorticity form)
Kópházi et al. (2009)	MSRE	3-D (neutronics) 1-D (thermal–hydraulics)	Transient Neutron kinetics + thermal–hydraulics coupled codes (DALTON + THERM)	Multi-group diffusion theory Homogeneous approach	Prescribed uniform velocity field Empirical correlation for heat transfer fuel/graphite
Zhang et al. (2009a)	Generic thermal MSR	2-D, axial-symmetric	Transient	Two-group diffusion theory Homogeneous approach	Prescribed uniform velocity field
Zhang et al. (2009b)	MOSART	0-D	Transient	Point-kinetics	Prescribed uniform velocity field Empirical correlation for heat transfer fuel/graphite
Zhang et al. (2009c)	Generic thermal MSR	2-D, axial-symmetric	Steady	Two-group diffusion theory homogeneous approach	Navier–Stokes equations (RANS/k–ε model)
This work	MSBR	2-D, axial-symmetric	Transient COMSOL Multiphysics®	Two-group diffusion theory Heterogeneous approach	Navier–Stokes equations (RANS/k–ε model)

for the model and are computed by means of the neutron transport code NEWT of SCALE 5.1 (DeHart, 2005a,b). To establish the potentialities of the proposed multi-physics modelling, a simplified geometry representing a typical channel of the MSBR core is considered. The MPM approach is applied to study the behaviour of the system in steady-state conditions and under several transients (i.e., reactivity insertion due to control rod movements, fuel mass flow rate variations due to the change of the pump working conditions, presence of periodic perturbations).

2. System description

In the present work, among the several Molten Salt Reactor concepts developed in the past and reconsidered in the last few years, the single-fluid MSBR proposed by ORNL in the 1970s (Robertson, 1971) was chosen as reference configuration. Because of its significant progress and the exhaustive information and data delivered by ORNL (Energy from Thorium), this reactor was considered (for instance, Křepel et al., 2007) as reference system for benchmark analyses and validation purposes in the framework of the EURATOM MOST project (Renault et al., 2005). The MSBR was designed to produce 2250 MW$_{th}$ and is featured by a thermal neutron spectrum and thorium fuel cycle (Fig. 1). The reactor has a central zone in which 13% of the volume consists of fuel salt (zone I), an outer, under-moderated region characterized by 37% of salt (zone II), and a reflector region containing about 1% of fuel – see Fig. 2a and b. The core is formed of square graphite-moderated blocks, each one with a central channel, through which the fuel salt flows (Fig. 2c). Interstitial flow passages are present between adjacent graphite elements so as to provide the required salt-to-graphite volume ratios (Robertson, 1971). The salt composition in the primary loop is the following: ^{7}LiF (71.7 mol%), BeF$_2$ (16 mol%), ThF$_4$ (12 mol%) and ^{233}UF$_4$ (0.3 mol%).

In this work, a single-channel of the MSBR core has been adopted for the analysis, with the aim to assess the potentialities of the developed multi-physics approach, focusing on the most relevant features related to the physical behaviour modelling, while neglecting the details of the actual geometrical domain. In particular, the effects of the square corners and interstitials have been disregarded, and a cylindrical geometry with axial-symmetric boundary conditions (leading to an infinite core in the radial direction) has been assumed for the modelled channel (Fig. 3), by keeping the same fuel to graphite volume ratio of the actual square graphite-moderated block. In this way, it has been possible to reduce the degrees of freedom of the problem instead of performing a complete 3-D simulation, which would have required a high computational cost.

The thermal–hydraulic parameters of the model have been chosen so as to reproduce the average conditions of zone I, which extends over the major part of the core (Robertson, 1971). The geometrical parameters and power densities have been calculated on the basis of a preliminary thermal–hydraulic analysis (Di Marcello, 2010), not reported here for brevity. The results are summarized in Table 2, whereas in Table 3 the main thermo-physical properties of fuel salt and graphite are shown.

3. The multi-physics model

The MPM approach, adopted in the present work for the analysis of the MSBR behaviour, consists of 14 coupled partial differential equations (PDEs), which have been implemented in the finite element COMSOL Multiphysics® software (COMSOL, 2008a) and allow the description of the coupling between neutronics and thermo-hydrodynamics in transient conditions. In the following, the models employed for the fluid flow, the heat transfer and neutronics, as well as the boundary conditions and neutron cross
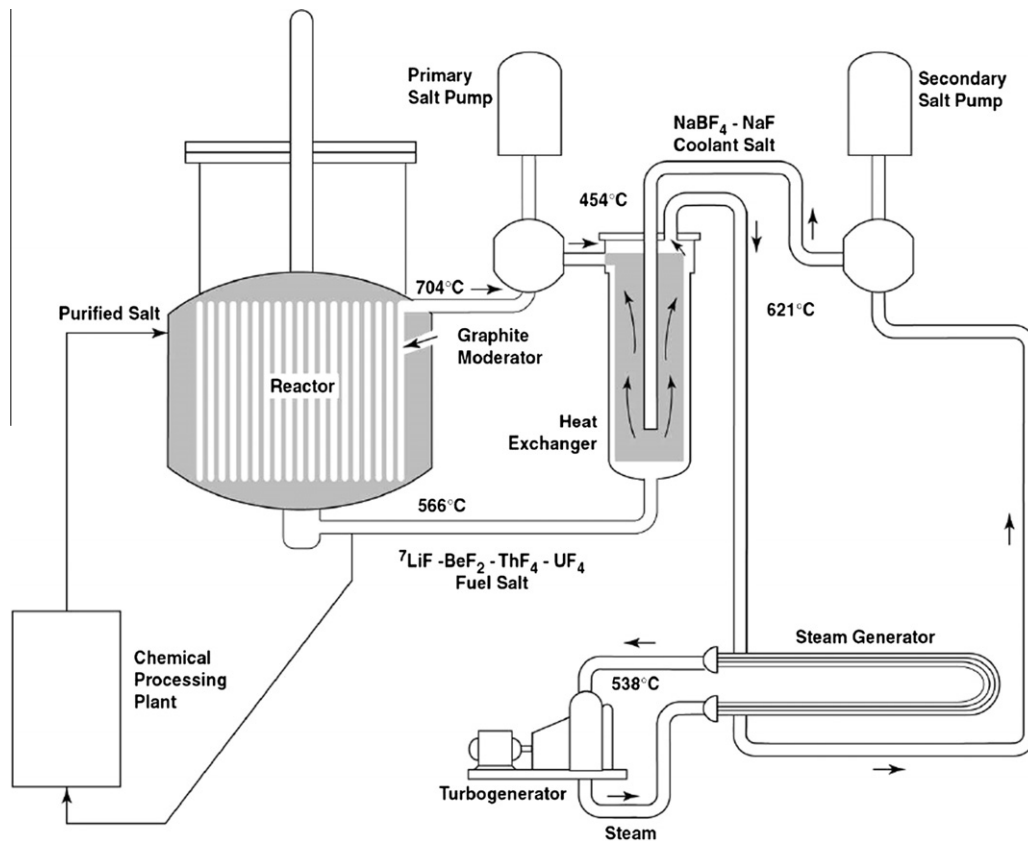

Fig. 1. Plant layout of the single-fluid Molten Salt Breeder Reactor.

section treatment, are presented. At the end of this section, the methods (among those available in COMSOL) employed in the present work for the numerical solution of PDEs both in steady-state and transient conditions are briefly described. Finally, a short summary of previous works performed for the assessment of the adopted models and for the validation of COMSOL numerical results is also given for completeness.

3.1. Fluid flow and heat transfer model

Great effort was spent by ORNL (Robertson, 1971) to identify the optimal core configuration in terms of diameter of the channels, since it affects several important design parameters, like the total feedback coefficient of reactivity, the breeding ratio, the neutron flux, the graphite life span and the fissile inventory (Mathieu et al., 2006; Forsberg et al., 2007). In particular, the MSBR channels are subjected to different thermal–hydraulic conditions, according to their position inside the core. Actually, very different channel diameters and velocities are found, so that the Reynolds number ranges approximately between 3×10^3 and 3×10^4. Corresponding to the calculated inlet flow velocity shown in Table 2, the Reynolds number is about 2×10^4, so that turbulent flow regime occurs. Hence, the incompressible form of the Reynolds Averaged Navier–Stokes (RANS) equations with Boussinesq's eddy viscosity hypothesis (Turner, 1973) is adopted considering the standard k–ε turbulence model (the empirical constants are given as $C_{\varepsilon 1} = 1.44$, $C_{\varepsilon 2} = 1.92$, $C_\mu = 0.9$, $\sigma_k = 1.0$, $\sigma_\varepsilon = 1.3$), according to Eqs. (1)–(4):

$$\rho_F \frac{\partial u}{\partial t} + \rho_F(u \cdot \nabla)u = F + \nabla \cdot \left[-pI - \frac{2}{3}\rho_F kI \right] + \nabla \cdot [(\eta + \eta_T)$$
$$\times (\nabla u + (\nabla u)^T)] \tag{1}$$

$$\nabla \cdot u = 0 \tag{2}$$

$$\rho_F \frac{\partial k}{\partial t} + \rho_F u \cdot \nabla k = \nabla \cdot \left[\left(\eta + \frac{\eta_T}{\sigma_k} \right) \nabla k \right] - \rho_F \varepsilon$$
$$+ \eta_T \left[\frac{1}{2} \left(\nabla u + (\nabla u)^T \right)^2 \right] \tag{3}$$

$$\rho_F \frac{\partial \varepsilon}{\partial t} + \rho_F u \cdot \nabla \varepsilon = \nabla \cdot \left[\left(\eta + \frac{\eta_T}{\sigma_\varepsilon} \right) \nabla \varepsilon \right] - \frac{C_{\varepsilon 2} \rho_F \varepsilon^2}{k} + C_{\varepsilon 1}$$
$$\times \frac{\varepsilon}{k} \eta_T \left[\frac{1}{2} (\nabla u + (\nabla u)^T)^2 \right] \tag{4}$$

As to the heat transfer, the energy balance equations (5) and (6) for the fuel salt and the graphite are adopted:

$$\rho_F C_{P,F} \frac{\partial T_F}{\partial t} + \nabla \cdot [-(K_F + K_T)\nabla T_F] = Q_F - \rho_F C_{P,F} u \cdot \nabla T_F \tag{5}$$

$$\rho_G C_{P,G} \frac{\partial T_G}{\partial t} + \nabla \cdot (-K_G \nabla T_G) = Q_G \tag{6}$$

It must be mentioned that natural convection can have a non-negligible effect on the fluid fuelled reactor dynamics, due to the large fuel salt expansion coefficient as demonstrated by Nicolino et al. (2008) and Křepel et al. (2007). Hence, the buoyancy effect due to gravity is taken into account through the volume force F into Eq. (1), as follows:

$$F_{//} = -g\alpha\rho_0(T_F - T_0), \quad F_\perp = 0 \tag{7a, b}$$

where the reference temperature T_0, the reference density ρ_0, and the coefficient of thermal expansion α of the fuel are calculated on the basis of ORNL evaluations (Robertson, 1971), and are given by $T_0 = 839$ K, $\rho_0 = 3374$ kg m^{-3}, $\alpha = 1.9857 \times 10^{-4}$ K^{-1}.

Molten salts are characterized by high molecular Prandtl numbers (Pr = 11, according to data reported in Table 2), therefore their heat transfer characteristics are slightly affected by the choice of the correlation for the turbulent Prandtl number, as extensively argued by Churchill (2002). In the analyses of the present work, the following correlation developed by Jischa and Rieke (1979) is adopted, since its form is to be preferred in terms of explicitness and simplicity:

$$\text{Pr}_T = 0.85 + 0.015/\text{Pr} \tag{8}$$

The heat source of the fuel salt in Eq. (5) depends on the neutron fission reactions and can be calculated from the neutron flux, as follows:

$$Q_F = \varepsilon_{f1}\Sigma_{f1}\phi_1 + \varepsilon_{f2}\Sigma_{f2}\phi_2 \tag{9}$$

As concerns the graphite, the heat generation (see Eq. (6)) is mainly induced by gamma heating and neutron irradiation (Robertson, 1971). This contribution is modelled assuming that the graphite heat source is a certain fraction of the fission energy released into the fuel, according to Eq. (10):

$$Q_G = \gamma \cdot Q_F \tag{10}$$

Such an approximation is generally employed in literature (Křepel et al., 2005; Zhang et al., 2009c). The graphite to fuel salt power density ratio (γ) has been evaluated on the basis of ORNL neutronic calculation results (Robertson, 1971). An average value for the zone I of the MSBR core is considered for the analyses and is given as $\gamma = 0.0144$.

3.2. Neutronics model

In order to treat the neutronic behaviour, the two-group diffusion theory is adopted. The velocity field of the fuel is taken into account by introducing a convection term in the balance equations of six families of delayed neutron precursors (DNP), whereas the neutrons are not affected by the molten salt motion because of the much shorter life span with respect to the characteristic time of the fuel circulation (Lapenta, 2005; Memoli et al., 2009). The neutron and precursors balance equations, in both the fuel and graphite material, are written in terms of fluxes and precursor concentrations as follows:

Fuel region
$$\begin{cases} \dfrac{1}{v_{1,F}} \dfrac{\partial \phi_1}{\partial t} = -\nabla \cdot (-D_{1,F}\nabla \phi_1) - (\Sigma_{a1,F} + \Sigma_{1 \to 2,F})\phi_1 + \Sigma_{2 \to 1,F}\phi_2 + (1-\beta)(v_1\Sigma_{f1}\phi_1 + v_2\Sigma_{f2}\phi_2) + \sum_{i=1}^{6} \lambda_i c_i \\[2mm] \dfrac{1}{v_{2,F}} \dfrac{\partial \phi_2}{\partial t} = -\nabla \cdot (-D_{2,F}\nabla \phi_2) - (\Sigma_{a2,F} + \Sigma_{2 \to 1,F})\phi_2 + \Sigma_{1 \to 2,F}\phi_1 \\[2mm] \dfrac{\partial c_i}{\partial t} = -\nabla \cdot (uc_i) + \beta_i(v_1\Sigma_{f1}\phi_1 + v_2\Sigma_{f2}\phi_2) - \lambda_i c_i \quad i = 1 \div 6 \end{cases} \tag{11}$$

Graphite region
$$\begin{cases} \dfrac{1}{v_{1,G}} \dfrac{\partial \phi_1}{\partial t} = -\nabla \cdot (-D_{1,G}\nabla \phi_1) - (\Sigma_{a1,G} + \Sigma_{1 \to 2,G})\phi_1 + \Sigma_{2 \to 1,G}\phi_2 \\[2mm] \dfrac{1}{v_{2,G}} \dfrac{\partial \phi_2}{\partial t} = -\nabla \cdot (-D_{2,G}\nabla \phi_2) - (\Sigma_{a2,G} + \Sigma_{2 \to 1,G})\phi_2 + \Sigma_{1 \to 2,G}\phi_1 \end{cases} \tag{12}$$
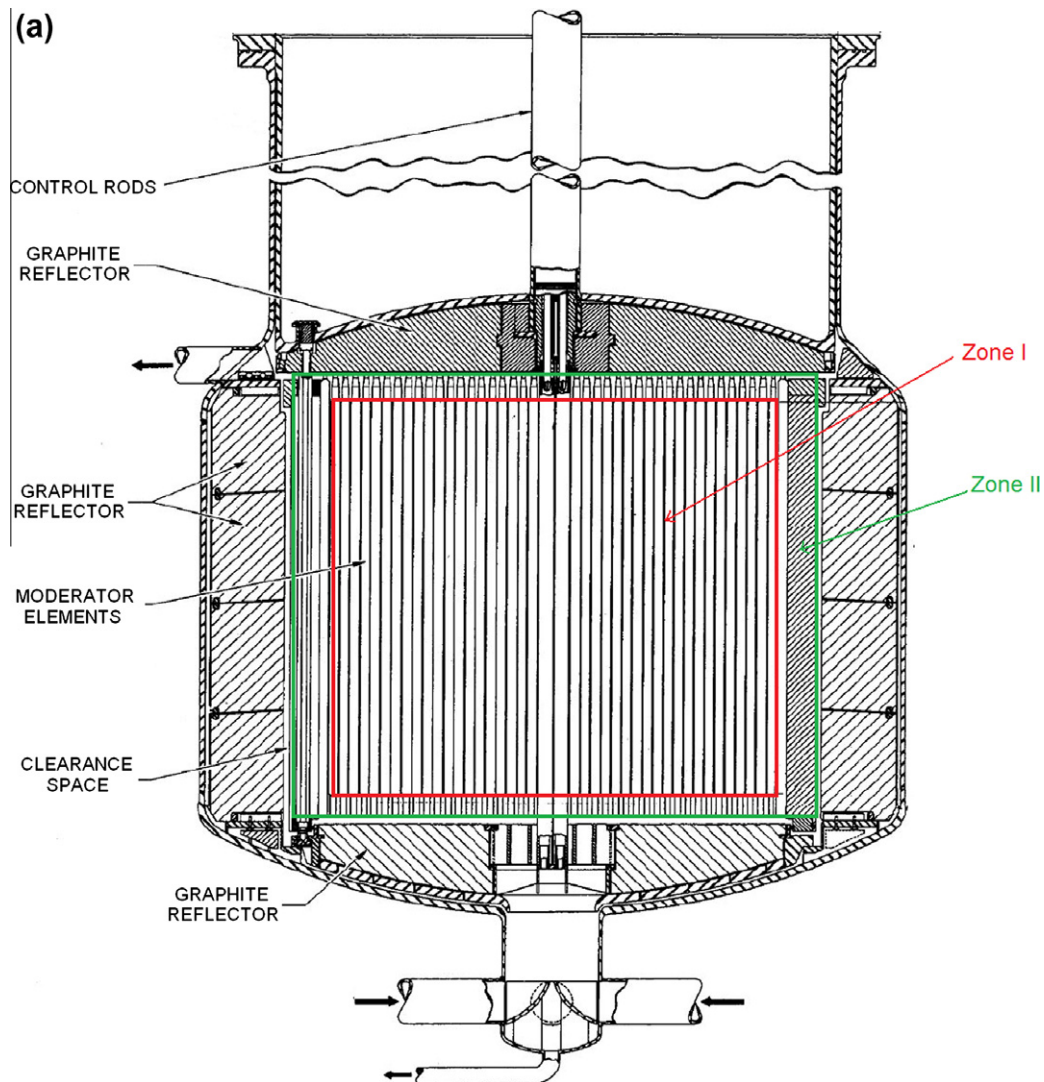
Fig. 2. (a) Vertical and (b) horizontal section of the MSBR core; (c) view of the graphite reflector and the moderated elements, showing in detail a graphite block of the central zone I and the presence of interstitials.

The above equation system is completed inserting a condition that takes into account the recirculation of the precursors (see Section 3.3).

The group constants (i.e., the cross sections and the diffusion coefficients) are usually calculated solving the neutron transport equation for infinite medium by means of a deterministic tool using a fine group cross-section library. The calculated neutron flux spectrum is then used to collapse the fine group cross sections. In the present work, the sequence NEWT of the modular system SCALE 5.1 (DeHart, 2005a,b) is chosen to perform this task using the standard cross section libraries ENDF/B-VI.7 (Bowman et al., 2005). In particular, NEWT solves the two-dimensional Boltzmann equation for neutrons employing the "extended step characteristic approach" (DeHart, 2005b). The adopted cell geometry for the group constant calculation is obtained taking into account the effective fuel to moderator volume ratio of the MSBR zone I. The fuel composition refers to the beginning of life (BOL), as reported in (Robertson, 1971), and therefore free of fission products. In order to allow for the neutron energy distribution distortion due to the axial neutron leak-age, the critical buckling correction (Lewis and Miller, 1984; DeHart, 2005b) is used in the solver.

3.3. Boundary conditions

The boundary conditions for the fluid flow, heat transfer and neutronic models are described here below, and represented in Fig. 3b and c.

3.3.1. Flow and heat transfer
As concerns the fuel salt, the following boundary conditions are imposed:

- *Inlet boundary*. The inlet velocity is given as $u_z = u_{in} = 1.47$ m/s and $u_r = 0$. The inlet values for the turbulent kinetic energy and the turbulent dissipation rate are prescribed according to the correlations suggested in (FLUENT, 2005), as follows: $k_{in} = 0.007$ m^2/s^2, $\varepsilon_{in} = 0.033$ m^2/s^3. $T_F = T_{in} = 839$ K is imposed to the inflow temperature.
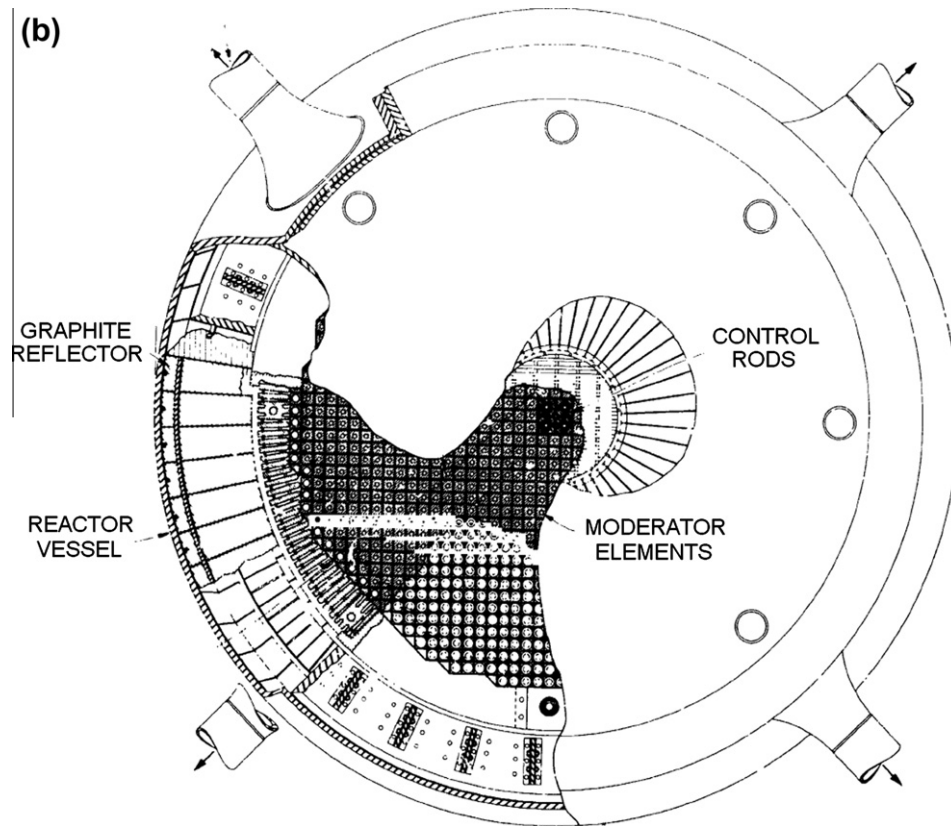
Fig. 2 (continued)

- *Outlet boundary.* The "local one-way method"[2] is exploited for $u, k,$ ε, and T_F, as generally used for outflow boundary conditions (Patankar, 1980).
- *Central boundary.* Symmetry conditions are considered on the axis of the channel.
- *Wall boundary.* The boundary condition at the interface between graphite and fuel salt is treated by means of the "wall function approach".[3]

As regards boundary conditions of the graphite domain, T_{in} is prescribed on the inlet boundary, while the insulation condition is used for T_G at the outlet boundary.

In order to take into account the effect of fuel flow through interstitials (see Section 2) on heat transfer, a further symmetry condition is assumed inside the graphite sub-domain ($r = R_G$) so as to obtain a more realistic temperature profile. The latter, because of the interstitials removing heat from the graphite, should present the maximum value ($dT/dr = 0$) approximately at the middle of the graphite sub-domain. While, by imposing a symmetry condition at the graphite axial boundary ($r = R_2$), the temperature profile would have the maximum at $r = R_2$, giving high discrepancies in the average temperature of the graphite between the actual channel and the modelled channel.

3.3.2. Neutron fluxes and delayed neutron precursors

- *Inlet boundary.* The "vacuum" boundary condition is adopted for the fast and thermal neutron fluxes at the inlet (i.e., $\varphi_1 = \varphi_2 = 0$), since the neutron extrapolation distance is negligible when compared to the axial dimension of the channel. The circulation of delayed neutron precursors is taken into account considering that a certain amount of DNPs can return into the core from the external loop according to their decay features, as follows:

$$c_{i,in}(t) = c_{i,out}(t - \tau_{EL})\exp(-\lambda_i \tau_{EL}) \tag{13}$$

- *Outlet boundary.* As at the inlet boundary, "vacuum" boundary condition is applied for fast and thermal fluxes at the outlet boundary, while the "local one-way method" is used for the delayed neutron precursors.
- *Wall and central boundaries.* Symmetry boundary conditions are imposed for the neutron fluxes at $r = 0$ and $r = R_2$. As concerns DNPs, the symmetry condition is chosen at $r = 0$, while the "impermeability" to fuel salt is considered at the wall ($r = R_1$).

As far as the interstitial effects are concerned, they are taken into account by keeping the same fuel to graphite volume ratio of the actual core channel. This assumption was verified in (Memoli et al., 2009).

3.4. Neutron cross sections

As concerns neutronics modelling, a set of temperature-dependent two-group cross sections are produced by means of SCALE 5.1, in the assumption of beginning of life fuel composition
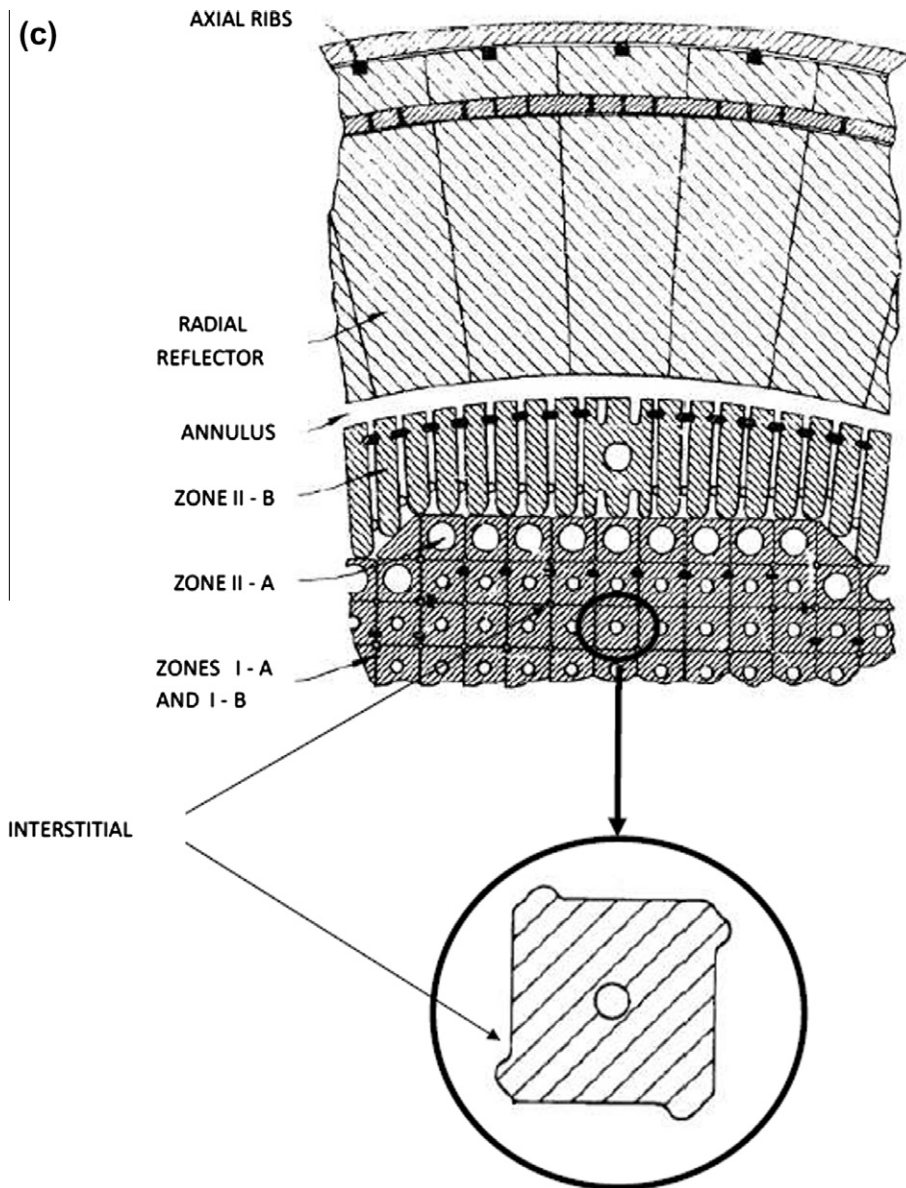
---

[2] The "local one-way method" consists in disregarding any boundary conditions in terms of velocity and temperature at the outlet boundary of the computational domain. This is appropriate when no re-circulating flow is expected, namely if there is a strong unidirectional flow in one direction that significantly influences the velocity field. In this case, the conditions at a point are largely affected by the upstream conditions, and very little by the downstream ones.

[3] The "wall function approach" consists in using empirically-based relations in turbulent flows near solid boundaries in order to describe the velocity and temperature profile in the thin boundary layer near the wall, instead of solving the turbulence equations.

Fig. 2 (*continued*)

(without fission products). They are included into the MPM approach as input parameters, so that no burn-up dependence of neutron cross sections is allowed for. Such an approximation can be considered acceptable in the case of MSRs because their neutronic characteristics are relatively independent of core lifetime (Suzuki and Shimazu, 2006, 2008). Infinite cell calculations by means of the transport code NEWT, using the 238 group cross-section library ENDF/B-VI.7, are carried out to generate a macroscopic cross section database under a discrete range of temperature of the fuel and the graphite region. The relationship between the group constants and the temperature is fitted in the following form:

$$\Sigma(T_F^{av}, T_G^{av}) = a_0 + a_1 T_F^{av} + a_2 T_G^{av} \qquad (14)$$

In this way, it is possible to take into account the heterogeneity of the MSBR channel. It is worth noting that the fuel salt and graphite temperatures are characterized by very different time constants during transients. A graphic representation of the fitted and calculated group constants as a function the fuel and graphite temperature is illustrated in Fig. 4.

A comparison of the feedback coefficients of fuel and graphite calculated by means of SCALE 5.1 and the diffusive model implemented in COMSOL are shown in Fig. 5, where COMSOL values are obtained performing eigenvalue calculations at different temperatures. In particular, the equation system defined by Eqs. (11) and (12) reduces to an eigenvalue problem in steady-state conditions (Bell and Glasstone, 1970), where the eigenvalues are the values of the multiplication factor (k) and eigenfunctions are the corresponding solutions for the neutron flux. If k_1 and k_2 represent the multiplication factors for temperatures T_1 and T_2, the feedback coefficient is given by $\alpha_T = (1/k_1 - 1/k_2)/(T_2 - T_1)$. As can be observed, a general good agreement can be found between the two approaches, and, in both cases, the calculated values do not significantly differ from those given by Křepel et al. (2007), who found salt and graphite temperature coefficients equal to −2.491 pcm/K and 2.259 pcm/K, respectively. A little discrepancy can be found in the fuel salt coefficient, since the diffusive model returns higher
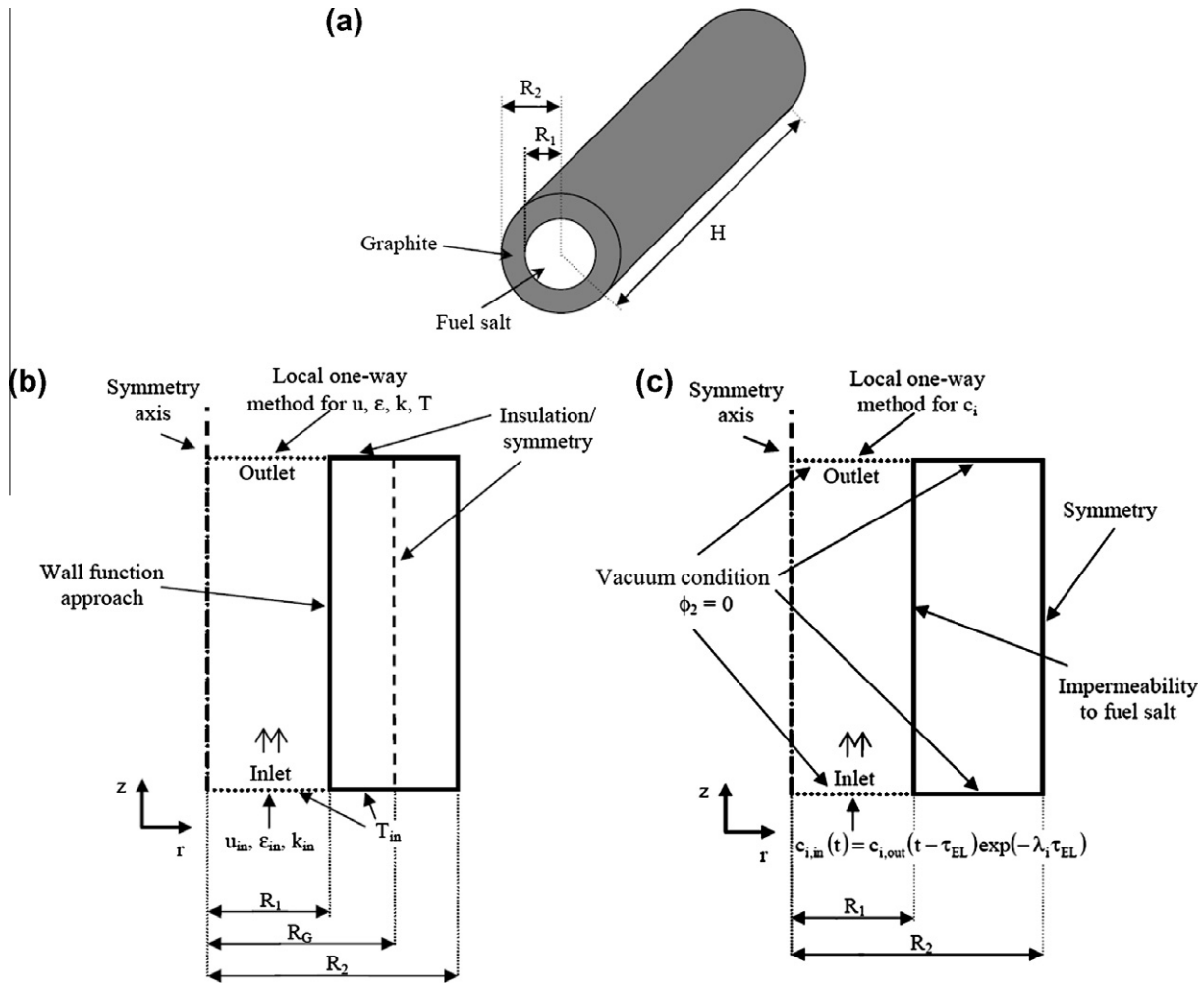
Fig. 3. (a) Geometrical representation of the analysed MSBR core channel; (b) fluid flow and heat transfer boundary conditions; (c) neutron flux and DNP boundary conditions.

Table 2
Main parameters of the analysed MSBR core channel.

Parameters	Values
Average power density (kW/l)	30.6
Average fuel salt power density (kW/l)	213.5
Average graphite power density (kW/l)	2.75
Channel radius, R_1 (m)	0.0208
Graphite outer radius, R_2 (m)	0.0573
Axial channel length, H (m)	3.96
Inlet fuel velocity (m s^{-1})	1.47
Inlet fuel temperature (K)	839
Outlet fuel temperature (K)	977
Volume fraction of fuel salt (%)	13.2
Graphite power density fraction to the total power (%)	9[a]

[a] Average value derived from ORNL calculations.

Table 3
Thermo-physical properties of fuel salt and graphite at 908 K.

Properties	Fuel salt	Graphite
ρ (kg m^{-3})	3327	1843
C_P (J kg^{-1} K^{-1})	1357	1760
K (W m^{-1} K^{-1})	1.23	31.2
η (kg m^{-1} s^{-1})	0.01	/

negative values than those calculated by SCALE 5.1. A reason of this discrepancy can be related to the fact that the SCALE 5.1 reactivity coefficients values are obtained by performing criticality cell calculation with a fixed buckling corresponding to the nominal height of the fuel channel. In this case, the reference value (i.e., the multiplication factor at the nominal temperature of fuel and graphite) is about 1.04. The reactivity coefficients, which come out of this calculation, are then relative to a non-critical spectrum, unlike the COMSOL values, which are calculated using two-group cross sections obtained by collapsing the fine group library over a critical spectrum.

3.5. Thermo-physical properties

Thermo-physical properties dependent on the temperature are necessary in the coupling analysis and calculation. Several experimental investigations were carried out at ORNL during the 1960s and 1970s to study the thermo-physical properties of different salt mixtures and graphite types. As concerns MSBR materials, a wide database is available and can be found in the documentation recently declassified by ORNL (Energy from Thorium). The correlations regarding density and viscosity of fuel salt and the graphite thermal conductivity are taken from (Robertson, 1971) and are expressed by Eqs. (15)–(17), respectively. As regards fuel salt thermal conductivity, experimental data reported in (Rosenthal et al., 1970a) have been fitted by the authors and the resulting expression is given by Eq. (18).
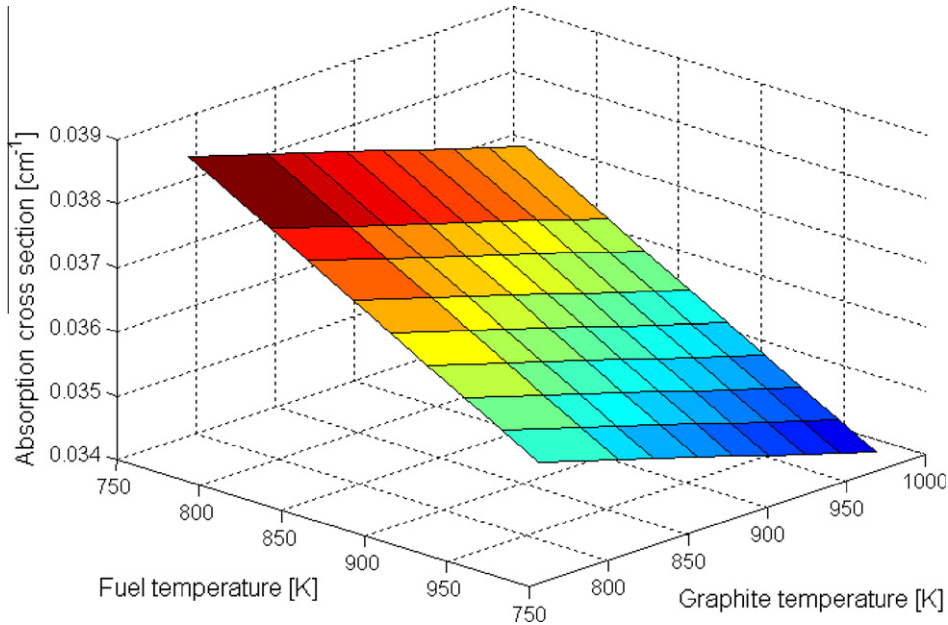
Fig. 4. Fuel absorption macroscopic cross section as a function of fuel and graphite temperature.

$$\rho \ [\text{kg/m}^3] = 3374\left(1 - 1.9857 \times 10^{-4}(T_F \ [\text{K}] - 839)\right) \tag{15}$$

$$\eta \ [\text{kg/m s}] = 0.109 \times 10^{-3} \cdot \exp(4090/T_F \ [\text{K}]) \tag{16}$$

$$K_G \ [\text{W/m K}] = 3763 \cdot (T_G \ [\text{K}])^{-0.7} \tag{17}$$

$$K_F \ [\text{W/m K}] = -3.70 \times 10^{-6} \cdot T_F^2 \ [^\circ\text{C}] + 4.77 \times 10^{-3} \cdot T_F \ [^\circ\text{C}] - 0.309$$
$$500 \,^\circ\text{C} \le T_F \le 900 \,^\circ\text{C} \tag{18}$$

The other thermo-physical properties of the fuel salt and graphite are assumed constant, and are given in Table 3.

3.6. Method of numerical solution

The solver used for the resolution of the PDE system adopted in the multi-physics model is based on the finite element method using quadratic Lagrangian elements. A mapped mesh consisting of quadrilateral elements is used to discretize the geometrical sub-domains. The overall equation system is solved using a segregated solver and each group of variables is solved by means of the direct method UMFPACK, which is based on the unsymmetric-pattern multifrontal method and direct LU factorization (Davis, 2004). As for the time stepping, the backward difference approach is applied to integrate the time derivatives. In order to handle numerical instabilities, anisotropic diffusion and streamline diffusion Galerkin Least-Squares are used, respectively, in the precursor balance equation and in the thermal fluid dynamics of the molten salt domain (energy and k–ε balance equations). Details on the convergence criteria of the time-dependent solver and the segregated solver are discussed with more detail in the COMSOL Multiphysics® Reference Guide (COMSOL, 2008b).

As far as the steady-state solution (Section 4.1) is concerned, it is found by solving the time-dependent problem. Usually, the initial conditions are relatively far from the stationary solution. In the case of the MSBR, the system is intrinsically stable (Di Marcello, 2010), hence the time-dependent solution gives a transient at the end of which the solution stabilizes at a certain power level, generally not corresponding to the nominal value. To deal with such circumstance, an absorption cross section (Σ_{abs}) is used so as to vary
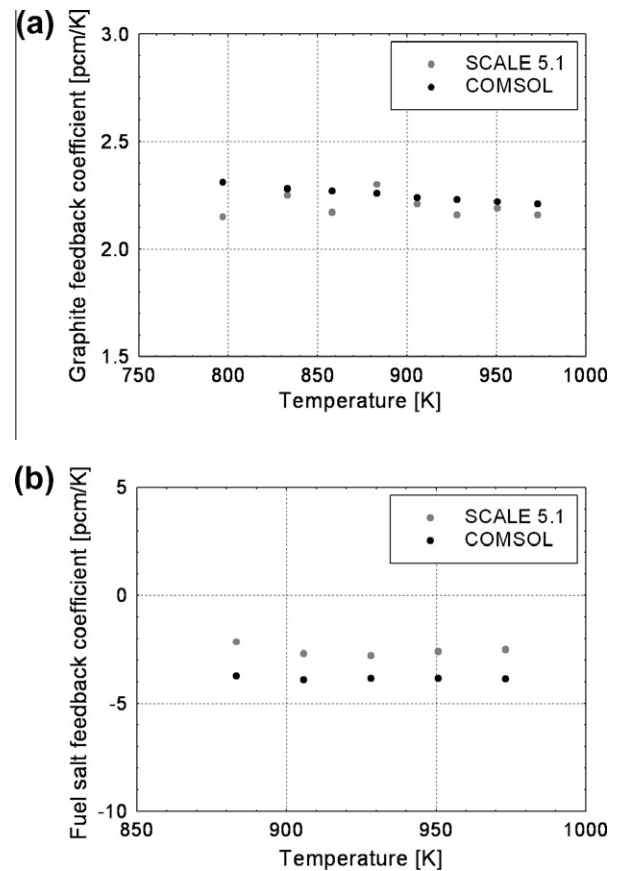

Fig. 5. Thermal feedback coefficients of graphite (a) and fuel salt (b) calculated by SCALE 5.1 and COMSOL.

the system reactivity and to bring the system at the nominal power level. In other words, the absorbing term Σ_{abs} is dynamically varied using a controller like a standard PID (Proportional–Integral–Derivative) configuration. At this point, once the power level is

reached, the solution is validated by performing a further eigen-value calculation, which returns a multiplication factor equal to 1 within the tolerance of the solver.

As concerns the power transients due to reactivity insertion (see Section 4.2.1), they are simulated by setting a certain value of the absorbing term Σ_{abs}, which can be considered as a diluted thermal neutron absorber and is introduced as control variable in order to adjust the neutron population according to the selected power level.

3.7. Validation of COMSOL numerical results

Great effort was spent at the Politecnico di Milano for the assessment of the results provided by COMSOL Multiphysics® (Cammi et al., 2007; Di Marcello et al., 2008; Cammi et al., 2009; Memoli et al., 2009; Luzzi et al., 2010). The thermo-hydrodynamics and neutronics models were tested independently, adopting differ-ent methodologies according to the peculiar characteristics occur-ring in MSRs.

As far as the flow and heat transfer modelling is concerned, a generalized analytic approach for pipe flow was developed in (Di Marcello et al., 2010), taking into account the fluid internal heat generation and incorporating recent developments in turbulence modelling (Churchill, 1997). This analytic solution was extended to take into account the heat conduction in the graphite moderator surrounding the fluid flow and considering the heat generation in-side the solid domain (Luzzi et al., 2010). The obtained overall ana-lytic solution (fluid fuel + graphite) was exploited to assess the COMSOL results exploring different Reynolds and Prandtl numbers and making also use of FLUENT (FLUENT, 2005) as a dedicated computational fluid dynamics code − for details see Cammi et al. (2009) and Luzzi et al. (2010).

A verification and validation of the neutronic model was carried both in the case of static and circulating fuel (Memoli et al., 2009). In the former, a code-to-code comparison between COMSOL, MNCP (Briesmeister, 2000) and SCALE 5.1 results was performed in terms of neutron flux, multiplication factor and macroscopic cross sec-tions. In the case of circulating fuel, a study of effective delayed neutron fraction as a function of fuel velocity was performed, and the results were compared with simplified neutron kinetics models (Memoli et al., 2009).

In all these works, COMSOL revealed an accurate and reliable tool. A general good agreement was found in all the comparisons, which can be considered acceptable from an engineering point of view.

4. Results and discussion

In this section, the MSBR behaviour in steady-state and tran-sient conditions is analysed by means of the proposed MPM ap-proach, with reference to the single-channel described in Section 2.

4.1. Steady-state conditions

The spatial distributions of the most relevant physical quanti-ties evaluated by means of COMSOL are described, since they give useful indications on the peculiar behaviour that is featured by the considered MSBR core channel, and more in general is typical of CFRs.

As concerns temperature profiles (Fig. 6), the results of present work are compared with the analytic solution developed in (Di Marcello et al., 2010; Luzzi et al., 2010) and used for validation (see Section 3.6). The comparison was performed in order to obtain an interpretation *a posteriori* of the model assumptions. Even if the
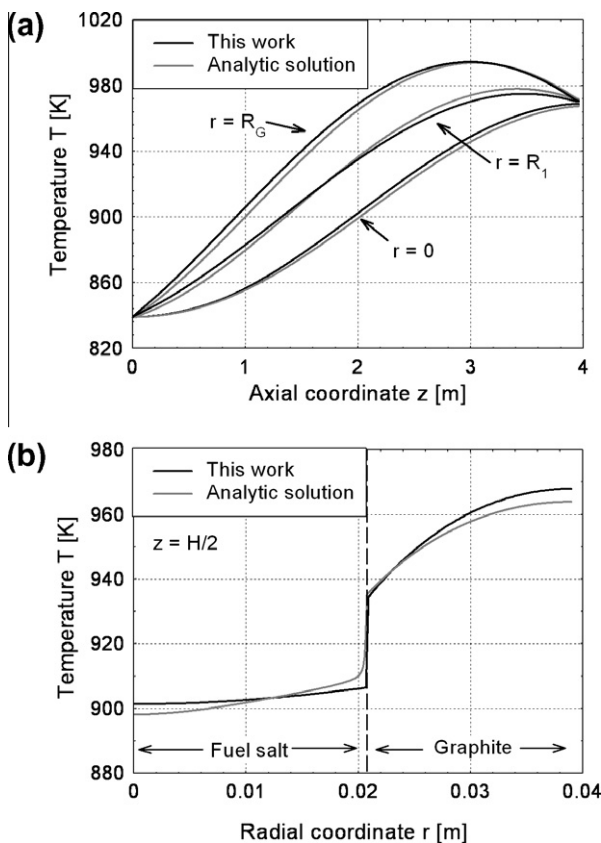

Fig. 6. Axial (a) and radial (b) temperature profiles in steady-state conditions.
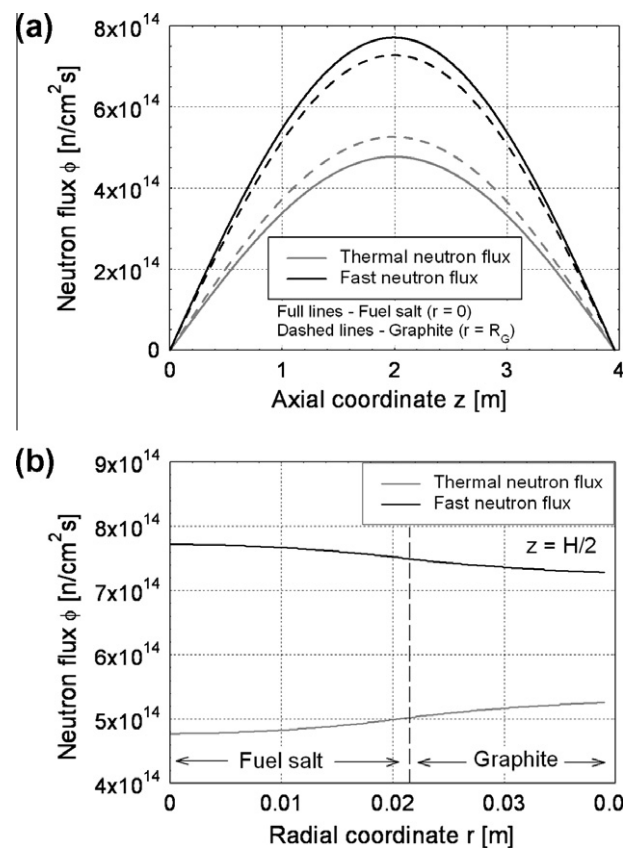

Fig. 7. Axial (a) and radial (b) neutron flux profiles in steady-state conditions.

analytic model applies under several assumptions (the temperature dependence of the thermo-physical properties is not considered, natural convection is neglected, and the fluid is in hydro-dynamically developed and thermally developing flow conditions), the discrepancies with the numerical results are kept down. This implies that the analytic solution is well representative of the temperature distribution and consequently of the velocity pattern occurring inside the core channel in steady-state conditions, and can be therefore used for a preliminary evaluation of the most important thermal–hydraulic parameters. In addition, the typical temperature trend of the MSR core channels is encountered (Fig. 6). The graphite is subjected to higher temperature with respect to the fuel salt, and the calculated values are in accordance with those given by ORNL (Robertson, 1971). Such behaviour is generally exhibited in steady-state conditions (Křepel et al., 2005), but during power transients the situation can be different (as shown in Section 4.2).

The calculated neutron fluxes are reported in Fig. 7. The fast neutron flux in the fuel results higher than that calculated in the graphite, since fission reactions can occur only in the molten salt. On the contrary, the thermal neutron flux is lower in the fuel zone with respect to the graphite moderator, analogously to solid-fuelled reactors.

DNP spatial distribution is a relevant feature of MSRs, and should be considered properly in the analyses. For instance, a zero-dimensional approach (by means of a zero-point neutron kinetics model) would lead to an underestimation of the reactivity loss due to fuel circulation (Kópházi et al., 2009; Memoli et al., 2009), with possible consequences on the system behaviour during transients. The present MPM approach allows to take into account the effects related to the spatial distribution of DNPs, both in steady-state and transient conditions. As concerns the former ones,

shown in Fig. 8, DNP concentration is strongly perturbed by the hydro-dynamic pattern inside the channel. In particular, precursors are more concentrated near the interface between fuel and graphite (i.e., where fuel velocity is lower), and in the upper zone of the channel.

4.2. Transient conditions

In this section, the proposed MPM approach is applied to study several transients driven by: (i) reactivity insertion due to control rod movements; (ii) fuel mass flow rate variations due to the change of the pump working conditions; (iii) presence of periodic perturbations.

4.2.1. Reactivity-driven transients

The first group of simulated transient conditions are driven by reactivity insertion due to control rod movements. This kind of transients is of specific interest for MSRs because the delayed neutron fraction is reduced, due to the loss of delayed neutrons in the external primary loop, and is smaller than that of other reactors (in which ^{235}U is commonly adopted), since ^{233}U is used as fissile material. Hence, an addition of positive reactivity could lead to a severe transient. In the following, reactivity prompt jumps up to 300 pcm are simulated starting from steady-state conditions at nominal power and nominal fuel flow rate.

The results in terms of power variations and temperatures of graphite and fuel salt are shown in Fig. 9. Power and temperature values encountered during the transients are strongly coupled each other. In particular, the power response of the system mainly depends on the negative salt reactivity feedback coefficient, which slows down the initial power fast growth. It can be noticed in
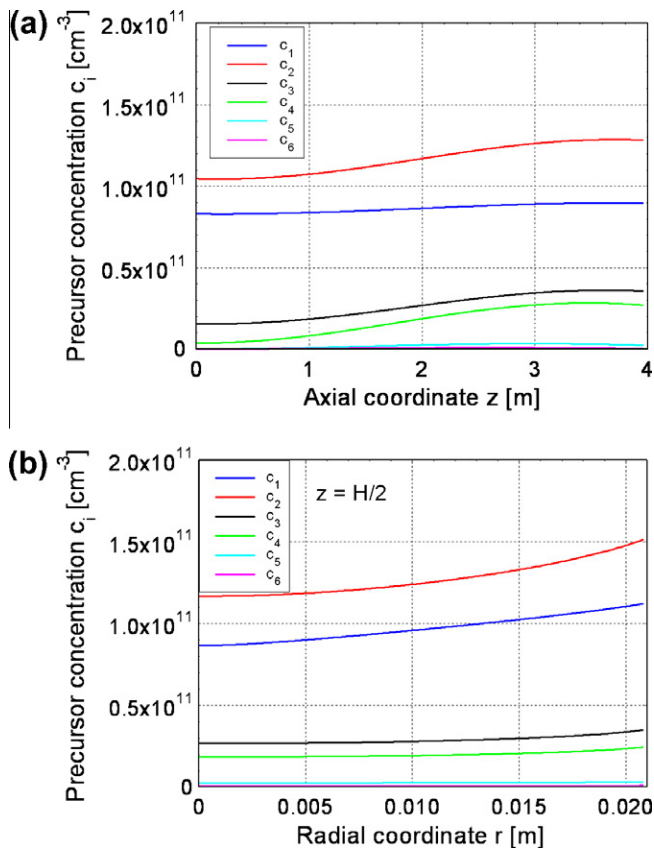

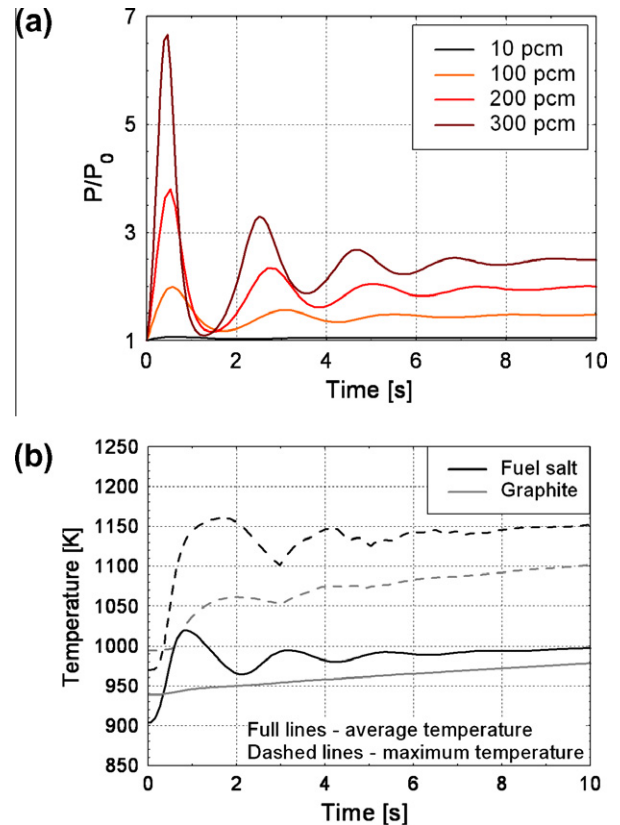**Fig. 8.** Axial (a) and radial (b) DNP profiles in steady-state conditions.

Fig. 9. Response of the MSBR core channel to the reactivity insertion with several reactivity levels at nominal power. The power (a) is shown for all reactivity levels. The temperatures (b) are given only for 300 pcm insertion results.
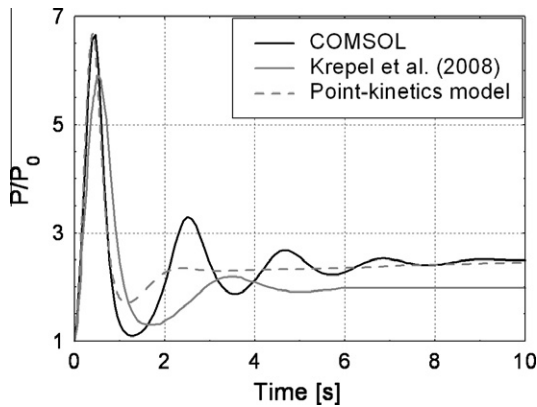
Fig. 10. Comparison between present results, those obtained by Křepel et al. (2008), and a point-kinetics model, in terms of system response to the reactivity insertion of 300 pcm.

Fig. 9b that the fuel experiences higher temperatures than the graphite moderator, differently from steady-state conditions. This behaviour is due to the strong difference between fuel salt and graphite time constants and represents a specific feature of MSR dynamics, unlike conventional solid-fuelled reactors. Actually, at the beginning of the transient, the heat is transferred from graphite to fuel salt (like in steady-state conditions), but a situation is reached with the radial heat flux inverted between them, due to the fast time response of the fuel.

From the safety point of view, the maximum temperatures reached by the fuel salt and graphite are fundamental parameters to be considered. In the case of 300 pcm reactivity jump, the greatest temperature is attained by the fuel maintaining an adequate safety margin with respect to the boiling temperature (about 1700 K). As concerns graphite, its temperature should be kept as low as possible due to undesired thermal expansion and increased thermal stresses, which can affect the performance of this component and its residual lifetime in reactor.

The achieved results are comparable with those obtained by Křepel et al. (2008), who performed the analysis of the entire MSBR core, as shown in Fig. 10, where also a point-kinetics model (whose parameters are chosen accordingly to the average conditions of the zone I of the MSBR core) is presented. Even if the analysed geometry is simplified, the model of the present work is well representative of the system behaviour in terms of power response. The discrepancies with respect to Křepel results in terms of peak and final power levels are due to the different system and geometry under consideration, namely: a representative channel of zone I of the MSBR core vs. the entire MSBR core. The additional piece of information of the proposed MPM approach arises from the possibility of describing the hydro-dynamic pattern. As a consequence, more pronounced oscillations in the power response are found, which cannot be caught by adopting a simplified thermal–hydraulic approach (one- or zero-dimentional) that leads to a more flat dynamic behaviour, as highlighted by the results of Křepel et al. (2008) and of a point-kinetics model.

4.2.2. Pump-driven transients

The second group of analysed transients is driven by the changing pumping rate. The system response is studied in the case of unprotected pump-driven transients (i.e., power is not maintained

by control rods) considering the following two situations: (a) pumping rate decrease of 80%; (b) pumping rate increase of 20%. The variations of fuel flow rate are simulated assuming an exponential response of the pump with a time constant of 2 s (Křepel et al., 2007).

The results in terms of power and temperature response are given in Fig. 11. The behaviour of the MSBR core channel is mainly governed by the feedback reactivity coefficient of the fuel salt, differently from the zero-power reactor dynamics (Křepel et al., 2008). It is worth mentioning that, because of the DNP drifting along the primary loop, pump flow rate increase causes DNP loss and induces negative reactivity, while pump flow rate decrease leads to positive reactivity. Fig. 11a denotes the power decrease at the transient beginning, and subsequently the stabilization at about the 35% of its initial value P_0. The decreasing fuel flow rate causes a rapid increase in the fuel temperature (Fig. 11b), which affects the power response through its feedback reactivity coefficients. The system response in the case of 20% increasing fuel flow rate (see Fig. 11c and d) is driven by a larger increase of graphite temperature (featured by a positive temperature feedback coefficient) with respect to that of fuel salt, leading to a positive reactivity insertion, and thus to an increase of power of about 25%.

The case of a decreasing pumping rate is of interest from the safety point of view, since it can give important information in the case of pump malfunctioning or in a more severe channel blockage in the reactor core. The strong increase of fuel and graphite temperatures shown in Fig. 11b can represent a dangerous condition for the MSBR, leading to possible local core damage in case of channel blockage (Křepel et al., 2008) if not prevented by the reactor safety systems.

4.2.3. Presence of periodic perturbations

The circulation of the fuel, besides the main effect of delayed neutron fraction reduction, can bring to periodic perturbations caused by local changes of the fuel properties. These local variations can then propagate throughout the whole primary loop. Examples of these perturbations are the formation of gas bubbles, which were experimentally detected in MSRE experience, and precipitation of fissile compounds, which can occur when fuel is added in excess with respect to the solubility limit in order to compensate burn-up effects. Dulla and Nicolino (2008) thoroughly analysed the problem of fissile compounds precipitation showing also the difference between a point-like approach and a three-dimensional one, considering the MSRE and MOSART systems. In the present work, fissile compound precipitation in the MSBR is studied. From the kinetic point of view, the main difference between the MSRE and MSBR is the presence in the latter of a positive thermal feedback of the graphite characterized by a large time constant (Mathieu et al., 2006).

To simulate the presence of a fissile lump in the channel, the fuel properties (represented by the macroscopic cross sections) are assumed to change according to a periodic square wave pulse. The spatial width of the pulse is given by the axial size of the lump and the amplitude is evaluated assuming that the fissile compound consists of UF_4, which is radially spread across the fuel channel. The period is given by the circulation time τ. In this way, the fuel two-group cross sections can be written according to Dulla and Nicolino (2008) as:

$$\Sigma_F(z,t) = \Sigma_F^0 + \delta\Sigma(z,t) \tag{19}$$

$$\delta\Sigma(z,t) = \begin{cases} b[\Theta(z - u_z(t-t_0)) - \Theta(z - u_z(t-t_0) - \Delta z)] & n \cdot \tau < t \leq n \cdot \tau + \tau_C \\ 0 & n \cdot \tau + \tau_C < t < (n+1)\tau \end{cases} \tag{20}$$
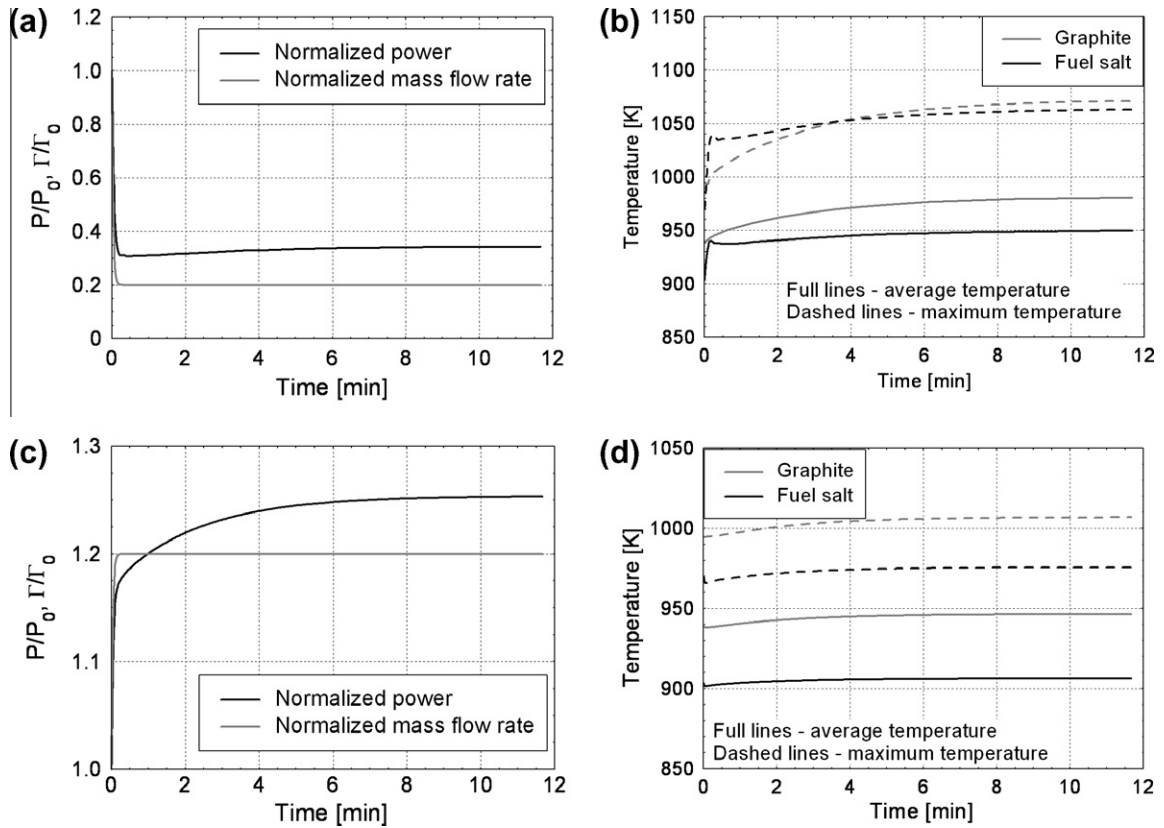
Fig. 11. Response of the MSBR core channel to fuel pump rate variations: power (a) and temperatures (b) response in case of 80% pump rate decrease; power (c) and temperatures (d) response in case of 20% pump rate increase.
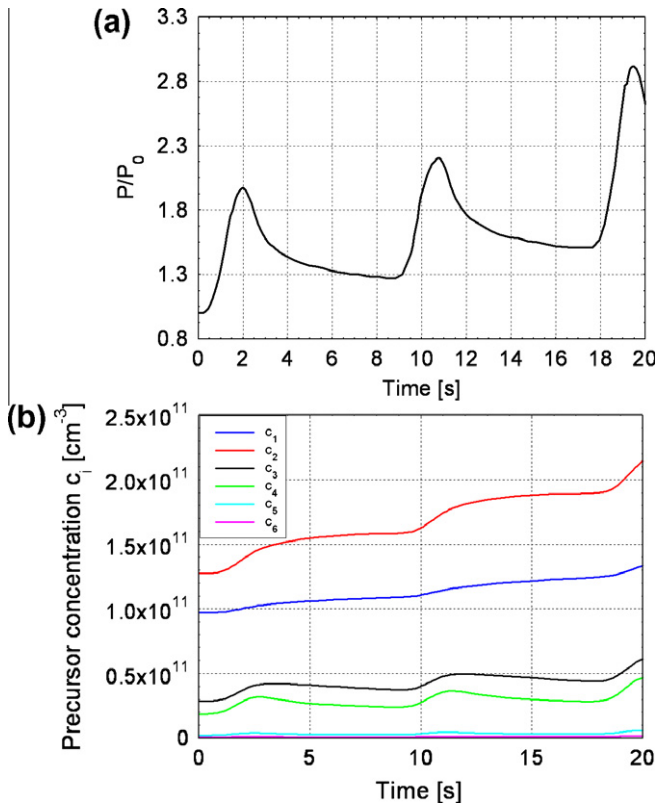

where b is the wave pulse amplitude (dependent on the cross sections of solid UF_4 and molten salt fuel), Θ is the Heaviside function, Δz is the axial size of the lump (equal to 5 mm in the considered analysis), and n is an integer number. The reactivity introduced into the system can be then adjusted for example by varying the UF_4 atomic fraction in the moving volume or the axial size itself. Collapsed cross sections for UF_4 are again calculated through the sequence NEWT of SCALE 5.1.

Zero-power and nominal power transients are considered. The zero-power transient refers to the case of a circulating fissile lump in the channel that gives a maximum total reactivity of 25 pcm. As shown in Fig. 12, during the fissile lump transit, lasting about 2 s,
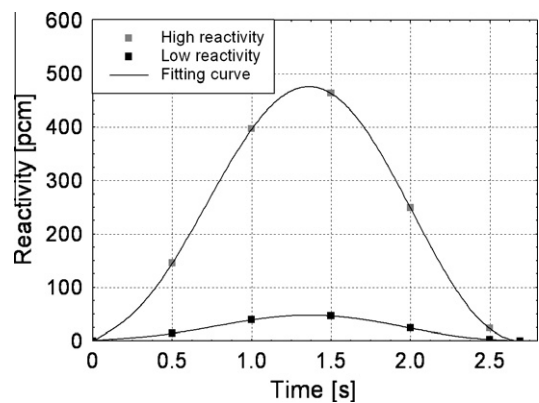
Fig. 12. System response to periodic perturbations (maximum total reactivity of 25 pcm) at zero-power in terms of power (a) and precursor concentration (b).

Fig. 13. Total reactivity behaviour during the lump transit in high and low reactivity cases.

the power is subject to a fast increase. When the fissile lump exits the channel, the power quickly decreases until the precursors (whose concentration builds up during the lump transit) start emitting delayed neutrons. As discussed by Dulla and Nicolino (2008), the zero-power dynamics is characterized by an asymptotic linear evolution of the power, which is clearly visible in Fig. 12.

The nominal power case is analysed for a maximum reactivity of about 50 pcm and 500 pcm, indicated in the following as low reactivity and high reactivity cases, respectively. The latter case (high reactivity) describes a super prompt critical configuration since the maximum reactivity insertion is larger than the value of β (about 300 pcm). Fig. 13 shows the total reactivity behaviour during the lump transit in both cases. The maximum value is reached, as expected, when the lump is in the mid channel (this occurs after about 1.3 s for the considered fuel velocity), where the adjoint fluxes reach the maximum values according to the perturbation theory (Lamarsh, 1966).

In Fig. 14, the system response of normalized power and precursor concentration for the case of 50 and 500 pcm, for the first three periods, is depicted together with the results achievable by means of a point-kinetics model. Besides the presence of large oscillations, with amplitudes up to 30% and 750% for low and high reactivity cases, respectively, both the power and the DNP concentration show a slight increase of the period averaged values. However, as found by Dulla and Nicolino (2008), differently from the zero-power case that is characterized by a divergent solution, the thermal feedback has the effect to stabilize the solution around a stationary value. The local perturbation of the neutron flux can be noticed in Fig. 15a, which shows the normalized fast and thermal flux axial profiles at different times during the lump transit for the high reactivity case. The solid fissile lump acts as a localized source of a fast neutrons, so that the fast flux shows a peak
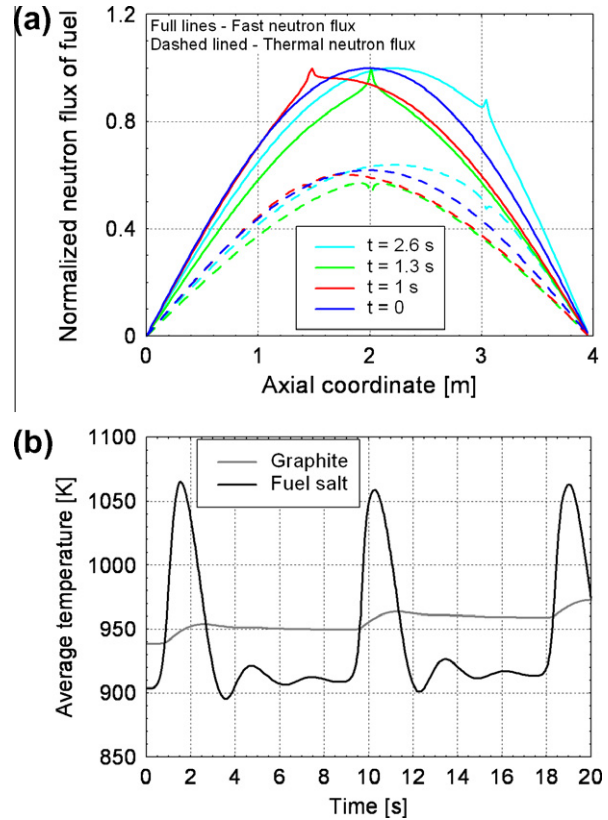

Fig. 15. Local perturbations of neutron fluxes at different times (a) and system temperature response (b) in the high reactivity case.
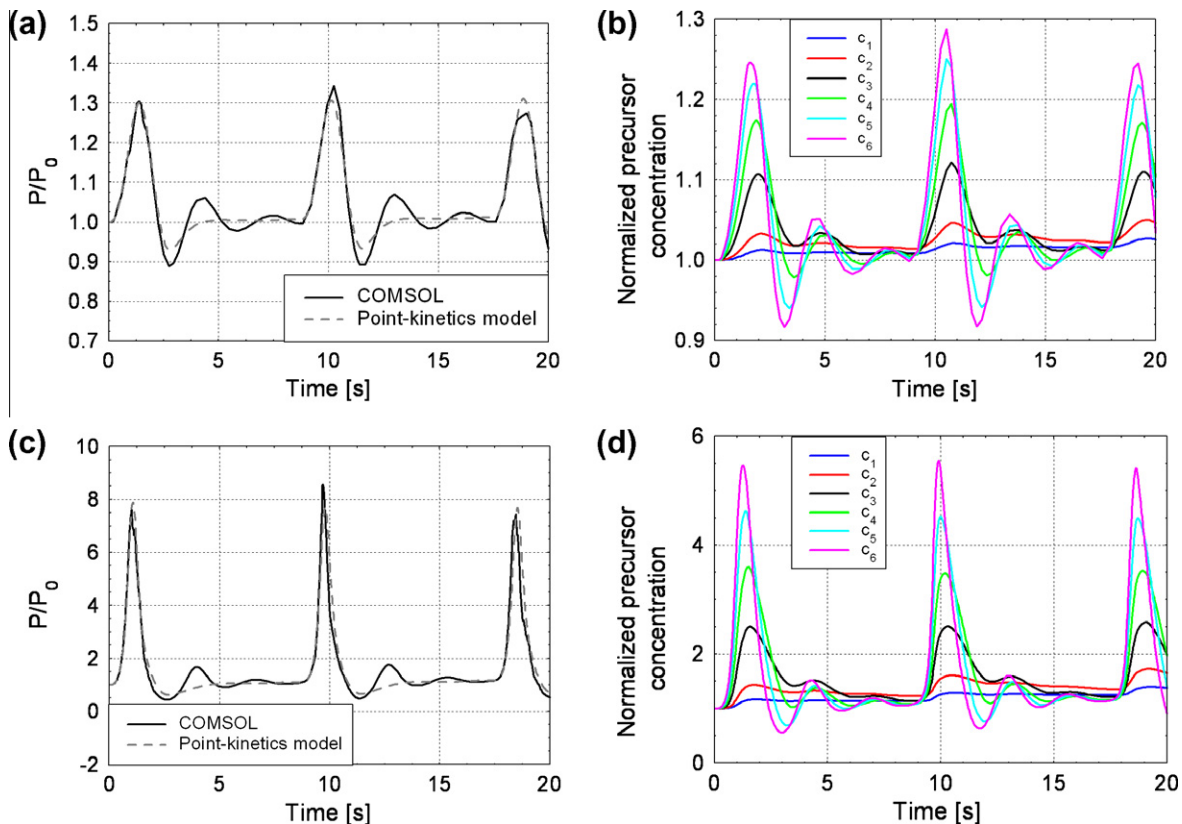

Fig. 14. System response to periodic perturbations at nominal power level in the low (a and b) and high (b and c) reactivity cases in terms of: (a–c) power where also the point-kinetics model is shown; (b–d) precursor concentration.

(Fig. 15a). On the other hand, a corresponding absorption of thermal neutrons occurs, so that the thermal flux shows a depression peak. This local perturbation is swept throughout the channel by the fuel velocity. For the same amount of reactivity, the average fuel and graphite temperature evolutions are shown in Fig. 15b. As already discussed, the fuel temperature presents a faster response to power change, whereas the graphite is subject to slow variation, being its time constant much greater than that of the fuel. Moreover, it is worth to note that also in the periodic perturbation analysis the description of the fluid motion by means of a fluid dynamics approach (allowing for turbulent phenomena) has relevant effect on the global behaviour. This behaviour presents indeed more pronounced oscillations with respect to more simplified thermo-hydraulic schemes, such as that offered by a point-kinetics model (Fig. 14a and b).

5. Conclusions

In this paper, a MPM approach for the analysis of the Molten Salt Reactor behaviour both in steady-state and transient conditions was presented. It allows to take into account the coupling (in space and time) between the several physical phenomena occurring in the reactor, whose interaction cannot be neglected when an accurate description of their dynamic evolution is required. In particular, the attention was focused on the interaction between neutronics and thermo-hydrodynamics. This is a well-known problem in nuclear engineering because it occurs with more or less evidence in conventional nuclear reactors, for which several coupling approaches are available in literature (e.g., the Coupled Code Technique between THSC and NKC). Differently from solid-fuelled reactors, MSRs are featured by an intrinsic coupling between neutronics and thermo-hydrodynamics (typical of circulating fuel systems), so that conventional approaches may result unpractical requiring strong modifications of the code numerical structure. In this framework, several studies were performed and different models and approaches can be found in literature. They provide a reasonable good description of the MSR behaviour, even if several simplifications (mainly on the thermo-hydro-dynamic modelling) are made. The MPM approach proposed herein is based on a different strategy, which adopts a multi-physics modelling (neutron diffusion theory + RANS + k–ε turbulence model + energy balance) in the unified environment of simulation offered by the finite element COMSOL software, which revealed flexible and robust at the same time. This approach has been applied to investigate the steady-state and transient conditions of the MSBR, with reference to a simplified geometry representing a typical core channel and suitable for the assessment of the most relevant features related to the physical behaviour modelling. It is worth noting that the developed MPM approach is of more general validity for studying the dynamic behaviour of other MSRs.

In particular, from the results achieved in this paper, the following main conclusions can be drawn.

1. The steady-state analysis has allowed to study the most relevant physical quantities (thermal and fast neutron flux, precursor concentration, graphite and fuel temperatures), by taking into account the spatial distribution of the coupled graphite-fuel salt system. As concerns heat transfer, the analytic solution developed at the Politecnico di Milano (Di Marcello et al., 2010; Luzzi et al., 2010) has offered a satisfactory interpretation *a posteriori* of the model assumptions, revealing as representative of the temperature distribution occurring inside the core channel, and useful for a preliminary evaluation of the most important thermal–hydraulic parameters.

2. Transient analyses have permitted to evaluate the system response in the case of reactivity-driven transients, pump-driven transients and presence of periodic perturbations, giving preliminary indications on safety related issues of MSRs, and more in general of circulating fuel systems. The comparison with the results obtained by Křepel et al. (2008) on the entire MSBR core, as well as with those achievable with a point-kinetics model, has demonstrated that: on one hand, the proposed MPM approach is representative and well descriptive of the MSBR core behaviour; on the other hand, the present model is able to give a significant additional piece of information on the system behaviour represented by the presence of further oscillations in the system response, thanks to the adoption of a more complete thermo-hydro-dynamic model with respect to one-dimensional flow models generally employed in literature.

All things considered, the present MPM approach is thought to be useful because: (i) neutronics and thermo-hydrodynamics are solved together in transient conditions, taking into account turbulence and buoyancy effects, as well as the heterogeneity of the system (in the calculation of group constants for molten salt and graphite); (ii) it provides additional information on the MSR dynamics, thanks to the accurate description of the fuel/coolant velocity pattern; (iii) it is in principle applicable to more complex geometries of MSRs, including the treatment of other "physics" (such as thermo-mechanics of structural components and/or permeation of fissile species and fission products through graphite), and can be used for control-oriented analyses, e.g. by means of the MATLAB/Simulink interface.

References

Bell, G.I., Glasstone, S., 1970. Nuclear Reactor Theory. Van Nostrand Reinhold Co., New York.
Bettis, E.S., Schroeder, R.W., Cristy, G.A., 1957. The aircraft reactor experiment – design and construction. Nucl. Sci. Eng. 2, 804–825.
Bowman, S.M., Dunn, M.E., Hollenbach, D.F., Jordan, W.C., 2005. Scale Cross Section Libraries. Technical Report, ORNL/TM-2005/39.
Briesmeister, J.F., 2000. MCNP – A General Monte Carlo N-Particle Transport Code. Technical Report, LA-13709-M, Los Alamos National Laboratory.
Cammi, A., Di Marcello, V., Fiorina, C., Luzzi, L., 2009. Assessment of COMSOL capabilities to analyse the thermo-hydrodynamic behaviour of the MSR core. In: Proceedings of the COMSOL Conference 2009, Milan, Italy, CD-ROM, COMSOL, Inc.
Cammi, A., Di Marcello, V., Luzzi, L., 2007. Modelling of circulating nuclear fuels with COMSOL Multiphysics. Proceedings of the European COMSOL Conference 2007, Grenoble, France, vol. 1. COMSOL, Inc., Berlin, pp. 380–386.
Cammi, A., Luzzi, L., 2008. Innovative techniques for the simulation and control of nuclear power plants. In: Durelle, V.B. (Ed.), Nuclear Energy Research Progress. Nova Science Publishers, pp. 1–4.
Churchill, S.W., 1997. New simplified models and formulations for turbulent flow and convection. AIChE J. 43 (5), 1125–1140.
Churchill, S.W., 2002. A reinterpretation of the turbulent Prandtl number. Ind. Eng. Chem. Res 41 (25), 6393–6401.
COMSOL Multiphysics® 3.5a USER'S Guide, 2008a. COMSOL Inc.
COMSOL Multiphysics® 3.5a Reference Guide, 2008b. COMSOL Inc.
Davis, T.A., 2004. Algorithm 832: UMFPACK, an unsymmetric-pattern multifrontal method. ACM Trans. Math. Software 30 (2), 196–199.
DeHart, M.D., 2005a. TRITON: A Two-dimensional Depletion Sequence for Characterization of Spent Nuclear Fuel. Technical Report, ORNL/TM-2005/39.
DeHart, M.D., 2005b. NEWT: A New Transport Algorithm for Two-dimensional Discrete Ordinates Analysis in Non-orthogonal Geometries. Technical Report, ORNL/TM-2005/39.
Di Marcello, V., 2010. Development of a Multi-physics Approach to the Modelling and Analysis of Molten Salt Reactors. Ph.D. Thesis, Politecnico di Milano.
Di Marcello, V., Cammi, A., Luzzi, L., 2008. Analysis of thermal-hydraulic behaviour of the molten salt nuclear fuel. In: Proceedings of the International Conference Nuclear Energy for New Europe 2008, Portorož, Slovenia, pp. 301.1–301.10.
Di Marcello, V., Cammi, A., Luzzi, L., 2010. A generalized approach to heat transfer in pipe flow with internal heat generation. Chem. Eng. Sci. 65, 1301–1310.
Dulla, S., Nicolino, C., 2008. Dynamics of fluid fuel reactors in the presence of periodic perturbations. Sci. Technol. Nucl. Instal. 2008, 1–11.
Dulla, S., Ravetto, P., 2007. Interactions between fluid-dynamics and neutronics phenomena in the physics of molten-salt systems. Nucl. Sci. Eng. 155, 475–488.

Dulla, S., Ravetto, P., Rostagno, M.M., 2004. Neutron kinetics of fluid-fuel systems by the quasi-static method. Ann. Nucl. Energy 31, 1709–1733.

Energy from Thorium. Documents Related to Liquid-halide (Fluoride and Chloride) Reactor Research and Development. In: <http://www.energyfromthorium.com/pdf/>.

FLUENT® 6.2 User's Guide, 2005. Fluent Inc.

Forsberg, C.W., Peterson, P.F., Pickard, P.S., 2003. Molten-salt-cooled advanced high-temperature reactor for production of hydrogen and electricity. Nucl. Technol. 144, 289–302.

Forsberg, C., Renault, C., Le Brun, C., Merlet-Lucotte, E., Ignatiev, V., 2007. Liquid salt applications and molten salt reactors. In: Proceedings of the 7th International Congress on Advances in Nuclear Power Plants (ICAPP '07), Nice, France.

Furukawa, K., Arakawa, K., Erbay, L.B., Ito, Y., Kato, Y., Kiyavitskaya, H., Lecocq, A., Mitachi, K., Moir, R., Numata, H., Pleasant, J.P., Sato, Y., Shimazu, Y., Simonenco, V.A., Sood, D.D., Urban, C., Yoshioka, R., 2008. A road map for the realization of global-scale thorium breeding fuel cycle by single molten-fluoride flow. Energy Convers. Manage. 49, 1848–1932.

Generation IV International Forum, 2002. A Technology Road Map for Generation IV Nuclear Energy Systems, GIF-002-00. Issued by the US DOE Nuclear Energy Research Advisory Committee and The Generation IV International Forum.

Generation IV International Forum, 2008. Gen IV International Forum 2008 Annual Report.

Hejzlar, P., Todreas, N.E., Shwageraus, E., Nikiforova, A., Petroski, R., Driscoll, M.J., 2009. Cross-comparison of fast reactor concepts with various coolants. Nucl. Eng. Des. 239, 2672–2691.

Hron, M., Uhlìr, J., Renault, C., 2006. "Molten salt reactor" current status and future prospects within European activities (MSR). In: Proceedings of FISA 2006 – Conference on EU Research and Training in Reactor Systems, Luxembourg, 2006, pp. 270–286.

Jischa, M., Rieke, H.B., 1979. About the prediction of turbulent Prandtl and Schmidt numbers from modified transport equations. Int. J. Heat Mass Transfer 22 (11), 1547–1555.

Kópházi, J., Lathouwers, D., Kloosterman, J.L., 2009. Development of a three-dimensional time-dependent calculation scheme for molten salt reactors and validation of the measurement data of the molten salt reactor experiment. Nucl. Sci. Eng. 163, 118–131.

Křepel, U., Grundmann, J., Rohde, U., Weiss, F.P., 2005. DYN1D-MSR dynamics code for molten salt reactors. Ann. Nucl. Energy 32, 1799–1824.

Křepel, J., Rohde, U., Grundmann, U., Weiss, F.P., 2007. DYN3D-MSR spatial dynamics code for molten salt reactors. Ann. Nucl. Energy 34, 449–462.

Křepel, J., Rohde, U., Grundmann, U., Weiss, F.P., 2008. Dynamics of molten salt re actors. Nucl. Technol. 164, 34–44.

Lamarsh, J.R., 1966. Introduction to Nuclear Reactor Theory. Addison-Wesley Publishing Company Inc., Reading, Massachusetts.

Lapenta, G., 2005. Mathematical and numerical models for the coupling of neutronics and thermal-hydraulics in circulating fuel nuclear reactors. In: Nuclear Reactor Physics. CLUT, Turin, pp. 195–210.

Lapenta, G., Mattioda, F., Ravetto, P., 2001. Point kinetic model for fluid fuel systems. Ann. Nucl. Energy 28, 1759–1772.

LeBlanc, D., 2009. Molten salt reactor: a new beginning for an old idea. In: Proceedings of 17th International Conference on Nuclear Engineering (ICONE17), Brussels, Belgium.

Lecarpentier, D., Carpentier, V., 2003. A neutronics program for critical and nonequilibrium study of mobile fuel reactors: the Cinsf1D code. Nucl. Sci. Eng. 143, 33–46.

Lewis, E.E., Miller, W.F., 1984. Computational Methods of Neutron Transport. John Wiley and Sons, New York.

Luzzi, L., Cammi, A., Di Marcello, V., Fiorina, C., 2010. An approach for the modelling and the analysis of the MSR thermo-hydrodynamic behaviour. Chem. Eng. Sci. 65, 4873–4883.

Mathieu, L., Heuer, D., Brissot, R., Garzenne, C., Le Brun, C., Lecarpentier, D., Liatard, E., Loiseaux, J.M., Méplan, O., 2006. The thorium molten salt reactor: moving on from the MSBR. Prog. Nucl. Energy 48, 664–679.

Meem, J.L., 1964. Two Group Reactor Theory. Gordon and Breach Science Publishers Inc., New York.

Memoli, V., 2010. Modelling Approaches for Analysis of Innovative Nuclear Reactors. Ph.D. Thesis, Politecnico di Milano.

Memoli, V., Cammi, A., Di Marcello, V., Luzzi, L., 2009. A preliminary approach to the neutronics of the molten salt reactor by means of COMSOL Multiphysics. In: Proceedings of the COMSOL Conference 2009, Milan, Italy, CD-ROM, COMSOL, Inc.

Nicolino, C., Lapenta, G., Dulla, S., Ravetto, P., 2008. Coupled dynamics in the physics of molten salt reactors. Ann. Nucl. Energy 35, 314–322.

Patankar, S.V., 1980. Numerical Heat Transfer and Fluid Flow. Hemisphere Publishing Co., New York.

Renault, C., Delpech, M., Le Brun, C., Lecarpentier, D., Garzenne, C., Konings, R.J.M., Hosnedl, P., Matal, O., Uhlir, J., 2005. The MOST project: key-points and challenges for the feasibility of molten salt reactors. In: Proceedings of the International Congress Advances Nuclear Power Plants (ICAPP 05), Seoul, South Korea, Paper 5208.

Robertson, R.C., 1971. Conceptual Design Study of a Single-fluid Molten-salt Breeder Reactor. Technical Report, ORNL-4541.

Rosenthal, M.W., Briggs, R.B., Kasten, P.R., 1970a. Molten-salt Reactor Program Semiannual Progress Report. Technical Report, ORNL-4449.

Rosenthal, M.W., Kasten, P.R., Briggs, R.B., 1970b. Molten-salt reactors – history, status, and potential. Nucl. Appl. Technol. 8, 107–117.

Salah, A.B., Hamidouche, T., D'Auria, F., 2008. Application of best estimate computational tools for safety accident analysis in nuclear plants. In: LÃ-n, W. (Ed.), Energy Conversion: New Research. Nova Science Publishers, Hauppauge, NY (Chapter 4).

Suzuki, N., Shimazu, Y., 2006. Preliminary safety analysis on depressurization accident without scram of a molten salt reactor. J. Nucl. Sci. Technol. 43, 720–730.

Suzuki, N., Shimazu, Y., 2008. Reactivity-initiated-accident analysis without scram of a molten salt reactor. J. Nucl. Sci. Technol. 45, 575–581.

Turner, J.S., 1973. Buoyancy effects in fluids. Cambridge University Press, Cambridge.

Wang, S., Rineiski, A., Maschek, W., 2006. Molten salt related extensions of the SIMMER-III code and its application for a burner reactor. Nucl. Eng. Des. 236, 1580–1588.

Yamamoto, T., Mitachi, K., Ikeuchi, K., Suzuki, T., 2006. Transient characteristics of small molten salt reactor during blockage accident. Heat Transfer Asian Res. 35, 434–450.

Yamamoto, T., Mitachi, K., Suzuki, T., 2005. Steady state analysis of small molten salt reactor. JSME Int. J. Ser. B 48 (3), 610–717.

Zhang, D.L., Qiu, S.Z., Su, G.H., Liu, C.L., Qian, L.B., 2009a. Analysis on the neutron kinetics for a molten salt reactor. Prog. Nucl. Energy 51, 624–636.

Zhang, D.L., Qiu, S.Z., Su, G.H., 2009b. Development of a safety analysis code for molten salt reactors. Nucl. Eng. Des. 239, 2778–2785.

Zhang, D.L., Qiu, S.Z., Su, G.H., Liu, C.L., 2009c. Development of a steady state analysis code for a molten salt reactor. Ann. Nucl. Energy 36, 590–603.